THE ASTROPHYSICAL JOURNAL, 299:236–254, 1985 December 1

THE EVOLUTION OF ASYMPTOTIC GIANT BRANCH STARS IN THE LARGE MAGELLANIC CLOUD. II. SPECTROSCOPY OF A COMPLETE SAMPLE

NEILL REID[1]
University of Sussex and Royal Greenwich Observatory

AND

JEREMY MOULD
Palomar Observatory, California Institute of Technology
Received 1985 January 23; accepted 1985 May 29

ABSTRACT

We have obtained spectra of 113 asymptotic giant branch (AGB) star candidates constituting six magnitude-limited, area-complete samples in the outer regions of the northern LMC. Luminosity functions constructed from these data are well represented by an underlying intermediate-mass AGB population, the product of continuous star formation over the last 3–4 Gyr, supplemented in some areas by more massive red giant and supergiant stars, with a typical age of $\sim 10^8$ yr. Most stars with $-5 > M_{bol} > -5.5$ show evidence for dredge-up of *s*-process elements, as do a smaller proportion in the range $-4.5 > M_{bol} > -5$. Only 10% of our sample, however, are C stars, and these are concentrated toward the Bar of the LMC. We have found no evidence for envelope burning in any of the stars in our sample.

Subject headings: galaxies: Magellanic Clouds — stars: evolution — stars: late-type

I. INTRODUCTION

The final phases of nuclear burning for all but the most massive stars takes place on the second, or "asymptotic" giant branch (AGB). Ground-breaking work in this area has shown the range of astrophysical possibilities in this evolutionary phase, including carbon star formation, *s*-process element production, pulsation, and mass loss (Iben and Renzini 1983; Wood 1981; Blanco, McCarthy, and Blanco 1980; Renzini and Voli 1981; Mould and Aaronson 1979; Westerlund *et al.* 1978). But precisely which processes occur in what mass ranges and on what time scales remains unclear and in need of better definition.

With this in mind we undertook in Reid and Mould (1984, hereafter Paper I) to compile a complete sample of stars in the relevant region of the H-R diagram. We chose a field in the Large Magellanic Cloud. This sample was photometrically defined, in contrast to most previous surveys, which have isolated spectroscopically interesting or variable stars. Such a sample surely offers better prospects of outlining the normal behavior of stars in this evolutionary phase, as opposed to the behavior just of noteworthy stars (see also Frogel and Richer 1983). Some simple caveats include the assumption that the stars remain visible and stick to a coarsely defined giant branch.

In Paper I we found that the bolometric luminosity function of stars in this complete sample was incompatible with the most explicitly formulated theory of steady mass loss, for any simple assumption about the star formation history of the field. The theory predicted more luminous stars ($-5 > M_{bol} > -6.5$) than were observed. It was suggested that more rapid mass loss than is normally assumed (e.g., Renzini and Voli 1981; Mould and Aaronson 1982) was truncating the evolution of these stars of comparatively modest luminosities. Evidence in favor of this view is seen in the AGB tips of LMC globular clusters (Aaronson and Mould 1984; Weidemann 1984; Mould 1983*a*). Evidence against includes detection of the AGB limit in a sample of long-period variables in the LMC (Wood, Bessell, and Fox 1981).

To further this investigation, we decided to obtain spectra of our complete sample. Since this is impracticable in full, a complete subsample has been isolated—or, in fact, complete subsamples, since luminosity function variations were detected over the field in Paper I. In particular, we wish to examine to what extent different portions of the luminosity function are populated by stars showing the various manifestations of AGB processing in their envelopes.

II. OBSERVATIONS

The candidate LMC AGB stars forming the bulk of this survey are listed in Table 1. These stars represent complete samples from six $22' \times 22'$ fields (A–F) chosen to be representative of the different conditions prevalent throughout the LMC (north) field. Field A is in the outermost regions of the LMC halo, while field B lies close to the eastern edge of Shapley Constellation III. These fields contain our deepest samples, extending to a bolometric limit of $M_{bol} < -4$ (using the Paper I bolometric correction prescription). Field D lies midway between Constellation III and Henize N13, and our sample in this field covers all stars with $M_{bol} < -5$ (two stars); field C is due south of D, near the Bar; F is near NGC 1783 and Henize N13, and E is between N13 and the Bar. As in field D, we include all stars with $M_{bol} < -5$. A number of other candidate LMC AGB stars with $M_{bol} < -5$ were observed on a more random basis, and data for these stars, together with the standards, are listed in the Appendix. The LMC variables are drawn from a variable star search being carried out in this field (Reid and Glass, in preparation) and have not been previously observed spectroscopically. LMC R-1 and R-3 are two of the six stars detected on the *I*-band plates and not on the *V* (see Paper I).

We obtained spectroscopic observations of these stars at Las Campanas Observatory in 1983 October and at the Anglo-

[1] Visiting Astronomer, Las Campanas Observatory.

TABLE 1

LMC AREA COMPLETE SAMPLES

	STAR	R.A.	DEC	V	V-I	Na D	D(6180) TiO	D(6475) ZrO	D(5635) C2	D(7100) TiO	Sp	M(bol)	Vel	Remarks
A	LMC 1	5 40 24.7	-64 47 16	17.61	3.09	0.58	-0.02	-0.03	0.24	0.08	K4?	-3.9		low S/N, ctm?
	LMC 3	5 40 8.1	-64 55 26	17.26	3.18	0.16	0.54	0.08	0.03	0.47	M4	-4.3	399	trace ZrO
	LMC 4	5 39 41.2	-64 55 49	16.81	2.94	0.17	0.64	0.02	0.07	0.67	M5	-4.4	315	
	LMC 5	5 39 43.3	-64 50 2	16.25	2.05	0.13	0.39	0.07	0.04	0.33	M2	-3.9	318	
	LMC 6	5 39 29.8	-64 50 8	13.16	1.99	0.16	0.23	0.13	0.03	0.23	M0	-6.9	320	strong 6498 + 4554?
	LMC 7	5 39 23.3	-64 47 8	15.90	1.82	0.08	0.26	0.10	-0.01	0.18	M1	-4.0	296	
	LMC 8	5 39 31.5	-65 0 13	16.20	2.21	0.08	0.20	0.01	0.03	0.16	M0	-4.1	312	
	LMC 9	5 39 30.9	-65 0 3	16.42	2.28	0.25	0.48	0.03	0.11	0.40	M3	-4.0	291	
	LMC 11	5 39 10.2	-64 54 59	15.93	1.99	0.14	0.47	-0.01	0.05	0.44	M3	-4.1	353	
	LMC 15	5 38 53.1	-64 48 6	16.42	2.97	0.19	0.38	0.26	0.06	0.30	M2S	-4.9	321	
	LMC 16	5 38 39.6	-64 57 8	16.51	2.94	0.15	0.22	0.18	1.22	0.23	C	-5.1	314	
	LMC 18	5 38 35.7	-65 3 24	16.09	2.19	0.20	0.44	0.06	0.10	0.36	M2	-4.2	324	
	LMC 21	5 38 4.9	-64 49 8	16.42	2.97	0.09	0.58	0.35	0.04	0.45	M4S	-4.9	340	^{13}CN strong
	LMC 23	5 37 56.8	-64 56 44	14.77	1.61	0.67	0.17	0.00	0.00	0.07	K5V		11	
	LMC 24	5 37 51.2	-64 54 34	15.69	1.80	-0.01	0.15	0.09	0.06	0.11	K5	-4.1	287	Hα , V = 396
	LMC 25	5 37 47.3	-64 50 47	16.23	2.01	0.17	0.15	0.30	0.05	0.13	K5S	-3.8	281	
	LMC 28	5 37 46.4	-64 59 30	16.52	2.27	0.60	0.26	0.00	0.20	0.20	M1V		56	strong CaH
B	LMC 31	5 32 41.3	-66 50 44	15.38	1.74	0.10	0.08	0.04	0.00	0.06	K5	-4.4	355	
	LMC 33	5 32 39.3	-66 39 31	13.12	1.89	0.09	0.14	0.06	0.00	0.08	K5	-6.8	340	
	LMC 35	5 32 25.7	-66 32 43	17.37	3.66	0.12	0.57	0.20	0.16	0.57	M4S	-5.0	328	
	LMC 36	5 32 33.5	-66 32 14	14.94	1.69	0.09	0.03	0.08	-0.06	-0.06	K4	-4.8	311	
	LMC 37	5 32 31.2	-66 50 17	16.00	1.94	0.18	0.08	0.05	0.02	0.03	K5	-4.0	286	
	LMC 38	5 32 29.1	-66 48 43	13.42	2.05	0.17	0.20	0.12	-0.01	0.08	M0	-6.7	314	
	LMC 39	5 32 27.9	-66 48 15	15.38	1.69	0.17	0.10	0.06	-0.01	0.16	K5		30	galactic giant
	LMC 40	5 32 25.6	-66 47 28	12.78	1.66	0.10	0.13	0.11	-0.02	0.07	K5	-6.9	316	4554 Ba II ?
	LMC 42	5 32 12.3	-66 47 24	16.54	2.29	0.17	0.21	0.30	0.03	0.18	M0S	-3.9	292	
	LMC 45	5 32 7.8	-66 34 57	16.40	2.54	0.12	0.64	0.00	0.05	0.54	M5	-4.3	322	
	LMC 47	5 32 0.6	-66 44 16	15.64	2.29	0.19	0.31	0.09	0.12	0.28	M1	-4.8	329	trace ZrO
	LMC 48	5 31 57.0	-66 42 50	16.25	2.87	0.13	0.57	0.10	0.09	0.59	M4	-4.9	312	
	LMC 52	5 31 59.9	-66 31 11	15.22	2.18	0.12	0.46	0.08	0.09	0.35	M3	-5.0	357	strong 6498
	LMC 53	5 31 40.3	-66 32 18	13.90	1.63	0.10	0.06	0.07	0.04	0.05	K4	-5.8	346	
	LMC 55	5 31 40.8	-66 44 43	13.26	1.90	0.12	0.14	0.08	-0.02	0.12	K5	-6.7	320	
	LMC 56	5 31 35.7	-66 32 11	12.56	3.04	0.17	0.37	0.06	0.10	0.40	M2	-8.8	340	
	LMC 61	5 31 17.4	-66 40 51	16.08	1.97	0.09	0.16	0.05	0.07	0.13	M0	-3.9	289	
	LMC 63	5 31 13.2	-66 34 2	17.43	3.58	0.17	0.18	0.25	1.37	0.13	C	-5.2	324	
	LMC 64	5 31 7.1	-66 49 0	17.15	2.77	0.67	0.56	-0.07	0.11	0.51	M4V		53	
	LMC 65	5 31 3.5	-66 43 5	15.97	2.05	0.26	0.11	0.27	0.54	0.26	C	-4.1	392	
	LMC 68	5 30 57.6	-66 46 54	16.79	2.93	-0.04	0.73	-0.12	0.11	1.24	M6	-4.5	320	
	LMC 69	5 30 47.5	-66 45 23	12.11	2.25	0.17	0.34	0.07	0.08	0.32	M2	-8.2	355	
	LMC 71	5 30 34.8	-66 41 7	16.25	2.62	0.32	0.18	0.30	1.26	0.25	C	-4.8	314	
	LMC 77	5 30 27.0	-66 34 59	16.36	2.85	0.14	0.70	0.23	-0.07	0.41	M5S	-4.8	309	
	LMC 79	5 30 28.3	-66 33 32	11.52	1.66	0.11	0.03	0.06	-0.04	0.02	K4		52	galactic giant
	LMC 80	5 30 28.1	-66 32 10	16.57	2.51	0.07	0.11	0.09	-0.02	-0.04	K5	-4.1	346	Hα , V=421
	LMC 81	5 30 20.0	-66 51 25	16.17	2.37	0.20	0.32	0.13	0.09	0.22	M1	-4.3	316	6498
	LMC 82	5 30 21.4	-66 49 17	13.61	1.90	0.13	0.14	0.08	0.03	0.14	K5	-6.3	326	
	LMC 83	5 30 14.9	-66 46 46	16.56	2.26	0.15	0.40	0.11	-0.01	0.28	M2	-3.8	379	
	LMC 86	5 30 7.0	-66 46 40	16.38	2.62	0.12	0.43	0.13	0.06	0.33	M2	-4.4	338	trace ZrO
	LMC 87	5 30 8.0	-66 46 20	16.83	3.06	0.24	0.21	0.25	1.28	0.25	C	-5.0	277	
	LMC 89	5 30 1.4	-66 39 41	16.15	2.59	0.12	0.55	0.09	0.14	0.48	M4	-4.6	313	trace ZrO
	LMC 90	5 29 53.5	-66 44 17	16.37	2.84	0.18	0.56	0.31	0.11	0.54	M4S	-4.7	306	
	LMC 92	5 29 28.5	-66 49 58	13.40	1.90	0.14	0.14	0.07	0.00	0.12	K5	-6.5	289	
	LMC 94	5 29 25.6	-66 46 12	17.04	3.27	0.17	0.16	0.18	1.32	0.22	C	-5.1	305	
	LMC 95	5 29 22.4	-66 43 43	15.11	2.39	0.09	0.45	0.05	0.17	0.45	M3	-5.4	293	
	LMC 96	5 29 16.3	-66 41 44	15.14	1.62	0.07	0.03	0.07	0.00	0.05	K4	-4.5	282	
	LMC 98	5 29 1.4	-66 41 13	14.00	1.92	0.07	0.06	0.08	0.01	0.07	K4	-6.0	324	
	LMC 99	5 29 7.4	-66 38 15	15.04	2.84	0.04	0.01	0.06	0.06	-0.02	K4	-6.1	340	
D	LMC 122	5 20 45.6	-66 56 51	17.21	3.58	0.08	0.65	0.16	0.17	0.65	M5S	-5.0	272	
	LMC 129	5 20 11.2	-66 59 34	14.70	1.30	0.16	0.34	0.09	0.05	0.31	M2	-4.6	306	
	LMC 133	5 20 3.0	-66 58 3	14.08	1.79	0.13	0.14	0.06	0.08	0.06	K5	-5.7	320	
C	LMC 163	5 22 34.7	-68 13 10	13.84	1.67	0.34	0.12	-0.01	0.01	0.01	K4V		63	strong MgH
	LMC 166	5 22 29.1	-67 58 25	14.87	1.75	0.12	0.00	0.10	0.04	0.02	K4		-62	galactic giant
	LMC 167	5 22 27.7	-67 54 16	11.33	1.68	0.08	0.00	0.03	0.04	0.07	K4		24	G star
	LMC 168	5 22 24.0	-68 5 48	15.43	3.48	0.21	0.52	0.03	0.12	0.64	M3	-6.6	217	^{13}CN strong?
	LMC 170	5 22 23.2	-67 58 54	15.00	2.53	0.05	0.06	0.05	0.01	0.03	K4	-5.7	344	
	LMC 174	5 22 25.9	-67 52 21	16.80	3.25	0.22	0.58	0.06	0.09	0.47	M4	-4.9		
	LMC 191	5 21 46.2	-68 1 53	14.97	2.43	0.08	0.04	0.06	0.00	-0.02	K4	-5.6	327	
	LMC 201	5 21 27.2	-68 11 42	14.69	2.13	0.13	0.09	0.10	0.06	0.03	K5	-5.5	305	
	LMC 204	5 21 22.2	-68 2 33	14.87	2.34	0.10	0.06	0.05	0.01	0.04	K4	-5.6	333	
	LMC 213	5 20 33.2	-68 13 5	14.00	1.85	0.47	0.10	0.04	0.03	0.02	K4V		49	
	LMC 214	5 20 31.2	-68 12 3	14.43	1.73	0.11	0.05	0.05	-0.03	0.03	K4	-5.3	310	
	LMC 223	5 20 3.2	-68 6 58	12.54	2.98	0.15	0.29	0.10	0.04	0.27	M1	-8.8	301	
	LMC 224	5 20 8.0	-68 2 58	12.92	2.40	0.01	0.29	0.11	0.02	0.22	M1	-7.6	322	

Table 1—*Continued*

	STAR	R.A.	DEC	V	V-I	Na D	D(6180) TiO	D(6475) ZrO	D(5635) C2	D(7100) TiO	Sp	M(bol)	Vel	Remarks
	LMC 230	5 19 53.9	-68 5 22	13.59	2.24	0.16	0.26	0.09	0.02	0.21	M1	-6.7	322	
	LMC 242	5 19 27.5	-67 54 9	14.65	2.30	0.28	0.17	0.31	1.13	0.25	C	-5.8	293	
	LMC 243	5 19 33.5	-67 52 25	14.19	1.75	0.04	0.05	0.04	0.00	0.00	K4	-5.6	315	
	LMC 250	5 19 20.2	-68 1 49	16.19	3.12	0.21	0.56	0.01	0.03	0.68	M4	-5.3	316	
	LMC 256	5 19 5.1	-67 59 13	12.76	2.96	0.14	0.31	0.11	0.04	0.30	M1	-8.5		H_α, β, V=435
	LMC 264	5 18 40.8	-68 9 28	13.15	2.70	0.13	0.18	0.12	0.01	0.11	M0	-7.8	312	
	LMC 269	5 18 40.9	-67 56 30	16.39	2.92	0.03	0.61	0.10	-0.01	0.78	M4	-4.8	327	trace ZrO
F	LMC 280	5 4 15.4	-66 15 47	14.52	3.35	0.14	0.62	0.01	0.17	0.80	M4	-7.3	332	
	LMC 284	5 4 0.8	-66 17 50	12.94	1.97	0.12	0.15	0.10	0.03	0.09	K5	-7.1	307	
	LMC 285	5 4 3.8	-66 14 30	16.94	3.38	0.10	0.70	0.23	0.07	0.79	M5S	-5.0	323	
	LMC 286	5 4 11.0	-66 9 51	13.40	2.03	0.21	0.15	0.09	-0.02	0.09	K5	-6.7	331	
	LMC 289	5 3 54.0	-66 5 13	13.38	1.94	0.19	0.37	0.10	0.06	0.37	M2	-6.6	318	
	LMC 291	5 3 42.1	-66 8 2	12.74	1.75	0.19	0.17	0.10	0.04	0.14	M0	-7.0	306	
	LMC 293	5 3 30.1	-66 11 7	13.53	1.83	0.12	0.13	0.09	0.00	0.09	K5	-6.3	304	
	LMC 295	5 3 18.1	-66 17 19	13.33	1.65	0.14	0.06	0.07	0.03	0.06	K4	-6.3	327	
	LMC 298	5 3 28.4	-66 1 0	14.31	1.65	0.13	0.06	0.07	-0.02	0.01	K4	-5.4	320	
	LMC 300	5 3 9.2	-66 6 13	16.15	3.60	0.19	0.62	-0.06	0.24	1.03	M4	-6.1	293	
	LMC 301	5 2 58.2	-66 15 32	15.89	2.84	0.13	0.60	0.08	0.15	0.67	M4S	-5.2	283	
	LMC 302	5 2 51.9	-66 12 49	14.40	1.61	0.05	0.07	0.06	0.03	0.02	K5	-5.2	345	
	LMC 309	5 2 38.5	-66 2 33	13.59	1.65	0.09	0.13	0.06	-0.03	0.08	K5	-6.1	325	
	LMC 321	5 1 50.6	-66 6 38	13.61	1.97	0.11	0.17	0.08	0.01	0.14	M0	-6.4	333	
	LMC 322	5 1 37.7	-66 16 51	14.10	1.67	0.11	0.06	0.06	-0.01	-0.02	K4	-5.6	312	
	LMC 331	5 1 20.9	-66 7 46	14.02	2.08	0.14	0.32	0.06	0.04	0.26	M1	-6.1	346	
	LMC 338	5 1 7.8	-66 1 12	16.52	3.41	0.13	0.50	0.07	0.00	0.35	M3	-5.4	293	
	LMC 339	5 1 6.4	-66 0 59	15.16	1.93	0.25	0.91	0.03	0.36	1.27	>M6	-4.8	315	
E	LMC 341	5 4 12.4	-67 0 33	16.31	2.95	0.15	0.43	0.22			M2S	-5.0	296	
	LMC 345	5 4 8.9	-66 44 4	14.25	1.60	0.14	0.05	0.07			K4	-5.4	286	
	LMC 346	5 3 50.7	-67 4 10	12.95	1.63	0.56	0.16	0.04			K5V		17	
	LMC 349	5 4 1.9	-66 44 0	15.69	2.46	0.22	0.51	0.07			M3	-4.9	289	
	LMC 356	5 3 30.3	-66 57 50	15.84	2.66	0.36	0.17	0.33			C	-5.3	305:	
	LMC 357	5 3 22.3	-66 57 46	15.95	2.61	0.40	0.23	0.32			C	-5.1	284:	
	LMC 360	5 3 13.3	-67 3 33	15.75	2.60	0.25	0.28	0.00			M1	-5.0	300	
	LMC 369	5 3 10.0	-66 43 31	15.25	2.04	0.26	0.32	0.19			M1	-4.9	249	
	LMC 374	5 2 55.7	-66 47 32	13.75	1.63	0.48	0.12	0.11			K5V		6	
	LMC 390	5 2 17.8	-66 42 56	12.36	1.80	0.13	0.05	0.03			K4		57	galactic giant
	LMC 394	5 1 41.8	-67 2 9	15.41	2.27	0.35	0.12	0.31			C	-5.0	298	
	LMC 407	5 1 11.9	-67 0 13	14.31	1.71	0.29	0.45	0.14			M3	-5.4	279	
	LMC 410	5 1 24.2	-66 54 57	16.19	2.80	0.35	0.18	0.29			C	-5.2	327	
	LMC 415	5 1 15.0	-66 48 47	15.74	2.41	0.20	0.31	0.09			M1	-4.8	283	
	LMC 422	5 1 2.0	-66 49 45	18.18	4.37	0.26	0.90	0.10			>M6	-5.4		
	LMC 423	5 0 44.5	-66 58 22	16.82	4.29	0.42	1.00	0.03			>M6	-6.6	281	

Australian Observatory in 1983 November. At LCO we used the intensified Reticon detector and the Cassegrain spectrograph on the 2.5 m Du Pont telescope. With a 600 lines mm^{-1} grating blazed at 7500 Å, these data cover the wavelength range 4500–8000 Å at a resolution of 2.6 Å (3.0 channels). On most nights of the nine-night LCO run, seeing was 1″ or better, and we used a pair of 1″ × 2″ apertures throughout. Flat-field calibrations were taken at the beginning and end of each night's observations, and there is no evidence for significant variations during the run. Wavelength calibration is given by He-Ne-Ar arc spectra, which were obtained between LMC program star observations, allowing us to accurately correct for the infamous zero-point drift (e.g., Mould 1983*b*). For observations of standard stars, or in cases where the telescope was moved over substantial hour angles, we obtained standard arc calibration spectra both before and after the stellar observation. Cross-correlating 40 such pairs of arc spectra (from all nine nights) gives a mean difference of (0.34 ± 0.34) channels, equivalent to ~0.29 Å. This represents a measure of the uncertainty in the wavelength calibration of the LMC stars—all of which were calibrated against adjacent arcs.

The AAO observations were obtained using a 600 lines mm^{-1} grating, blazed at 6800 Å, with the 25 cm camera on the RGO spectrograph. An RCA 512 × 320 format CCD chip was used as the detector. These observations cover the wavelength range 5750–6800 Å, with a resolution of ~3.4 Å (1.″6 slit). Again, calibrating Cu-Ar arc spectra are interspersed between the LMC star observations and bracket each of the standard stars. Succeeding arcs generally agree to better than 0.1 pixels with a mean difference of 0.069 ± 0.092 pixels from 16 arc pairs (equivalent to 0.14 Å).

All these data were wavelength- and flux-calibrated using the Edinburgh Spectral Package on the STARLINK VAX 11/780 at RGO. As part of these reductions, the LCO data were rebinned from 3744 to 1872 channels by simply combining adjacent pixels. Flux calibration was relative to observations of the standard stars L745-46A (LCO, AAO), LTT 7987 (LCO), LTT 377 (AAO), and LTT 1020 (AAO) (Stone and Baldwin 1983; Baldwin and Stone 1984). L745-46A was used as the primary calibrator, with the other stars as independent checks. Our observations strongly suggest that the dip near 6800 Å in the Baldwin and Stone L745 calibration is not real, since incorporating this feature produces corresponding lumps in the other standard star spectra. L745-46A is a weak-lined DA white dwarf, and thus is unlikely to have spectral features at these wavelengths, and it is possible that the calibration

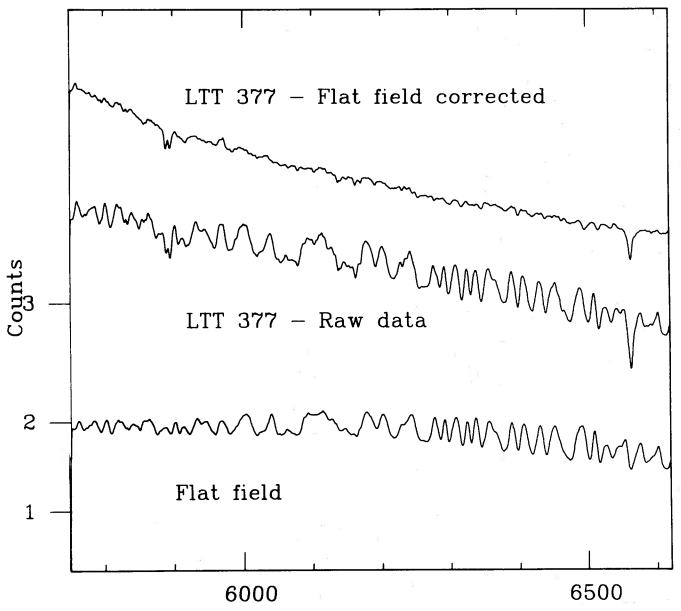

FIG. 1.—De-fringing of AAT CCD spectra. The fringe pattern on the RCA chip is corrected by dividing the raw stellar spectra by a normalized flat field. The flat-field corrected spectrum of LTT 377 illustrates the effectiveness of this technique.

reflects residual atmospheric absorption. In any event, we have chosen to linearly interpolate between Baldwin and Stone's measurements at 6600 and 7100 Å. Comparing with other standards, our final calibration appears reliable to $\lesssim 5\%$ in relative flux, although clearly the small slit size used rules out accurate absolute calibration.

The actual flux calibration was made by first dividing each spectrum with a normalized flat field and then applying the corrections for the wavelength sensitivity of the detector. This is straightforward for the LCO data but is complicated by the presence of strong fringe patterns on the thinned AAO CCD data. Flat-field frames were obtained using a dome screen illuminated by a tungsten lamp. Figure 1 presents spectra of LTT 377 before and after division by the flat field. Residual features are at the less than 5% level and are generally consistent with the level expected from the CCD readout noise combined with photon statistics. Typical examples of our final reduced spectra are displayed in Figure 2.

III. SPECTRAL CLASSIFICATION AND RADIAL VELOCITIES

a) Spectrophotometry

Our spectroscopic classification is based on a series of narrow-band photometric indices designed to act as sensitive luminosity and surface composition indicators. For each index we define a pseudo-continuum using two sidebands (see Table 2) and compare the predicted "continuum" flux with the observed flux in the central passband (cf. Mould 1976).

Table 1 presents the data for the individual LMC field stars. Apart from the spectroscopic indices, V magnitudes and $V-I$ colors (from the COSMOS data) are tabulated, as are bolometric magnitudes. Bessell and Wood have recently published bolometric corrections for K and M stars (Bessell and Wood 1984), and we have adopted their formula in preference to that of Paper I for M and S stars, viz.,

$$BC_I = 0.3 + 0.38(V-I) - 0.14(V-I)^2 ,$$

while we adopt

$$BC_I = 1.9 - 0.7(V-I)$$

for carbon stars. The latter is derived by combining Cohen *et al.*'s (1981) result $BC_I = 1.85 - 1.42(R-I)$ with the relation $(V-I) = 0.14 + 2.10(R-I)$ derived from Blanco and Richer's (1979) observations of C stars in NGC 419. The uncertainties in the latter calibration are at least 0.25 mag. In all cases, when applying these formulae a reddening of 0.125 mag (in $V-I$) is assumed.

The differences between Bessell and Wood's prescription and the bolometric calibrations adopted in Paper I are less than 0.1 mag for all save the reddest M stars ($V-I > 3$). Similarly, M_{bol} for carbon stars with $V-I < 2$ is little affected, but the luminosities of the redder carbon stars are progressively underestimated by the Paper I formalism. However, the spectroscopic results described below show that the latter stars make a relatively small contribution to the complete LMC AGB population.

Our classification system rests on the following indices, all of which are calibrated using the observations of the standard stars listed in the Appendix. The strength of the sodium D lines is used as a dwarf-giant discriminator. As Figure 3*a* shows, when plotted against $V-I$ (effective temperature), there is a tight sequence of M and S giants with low band strengths, with a few strong sodium line dwarfs and carbon stars. This criterion breaks down to some extent for $V-I > 4$, but overall this index is cleaner than classification using the CaH Dλ6830 index which we also computed. A number of the calibrating spectroscopic standards lack $V-I$ colors, and we have computed pseudo-$(V-I)$ colors using a continuum color $\langle 7500-5400\rangle$ with bandpasses of 140 Å centered on 5400 and 7500 Å. Figure 3*f* shows the relation between this color and $V-I$, and least-squares fitting gives a best-fit relation of

$$(V-I) = 1.36(\langle 7500-5400\rangle + 1.32)$$

with an rms scatter of 0.2 mag. These pseudo-$(V-I)$ colors are of greatest significance for the very red variables. The large discrepancies between photographic and spectroscopic values for these stars probably reflects the fact that the former are derived from 3V and 5I plates, poorly spaced in time, while the latter are simultaneous. Clearly our bolometric magnitudes cannot be regarded as reliable for these stars. Infrared JHK observations are essential in fixing their luminosities, and these are currently being obtained (Reid and Glass, in preparation).

Carbon stars amongst the LCO data are classified using the C_2 λ5635 band head (Fig. 3*b*). This index is not available for the AAO data, and C stars were identified from visual inspection of the spectra. (Note that since the LMC has a significant radial velocity [250 km s^{-1}] relative to the Sun, the bandpass

TABLE 2

NARROWBAND PHOTOMETRIC INDICES

Index	Sideband 1	Band	Sideband 2	Species
Dλ5635.....	5380–5400	5610–5630	5645–5665	C_2
Dλ5896.....	5845–5865	5880–5905	5940–5960	Na
Dλ6180.....	6056–6096	6165–6200	6580–6620	TiO
Dλ6270.....	6230–6255	6250–6275	6310–6330	^{13}CN
Dλ6475.....	6056–6096	6475–6510	6580–6620	ZrO
Dλ6708.....	6680–6697	6702–6712	6717–6731	Li
Dλ6830.....	6056–6096	6790–6870	7460–7540	CaH
Dλ7100.....	6056–6096	7060–7140	7460–7540	TiO

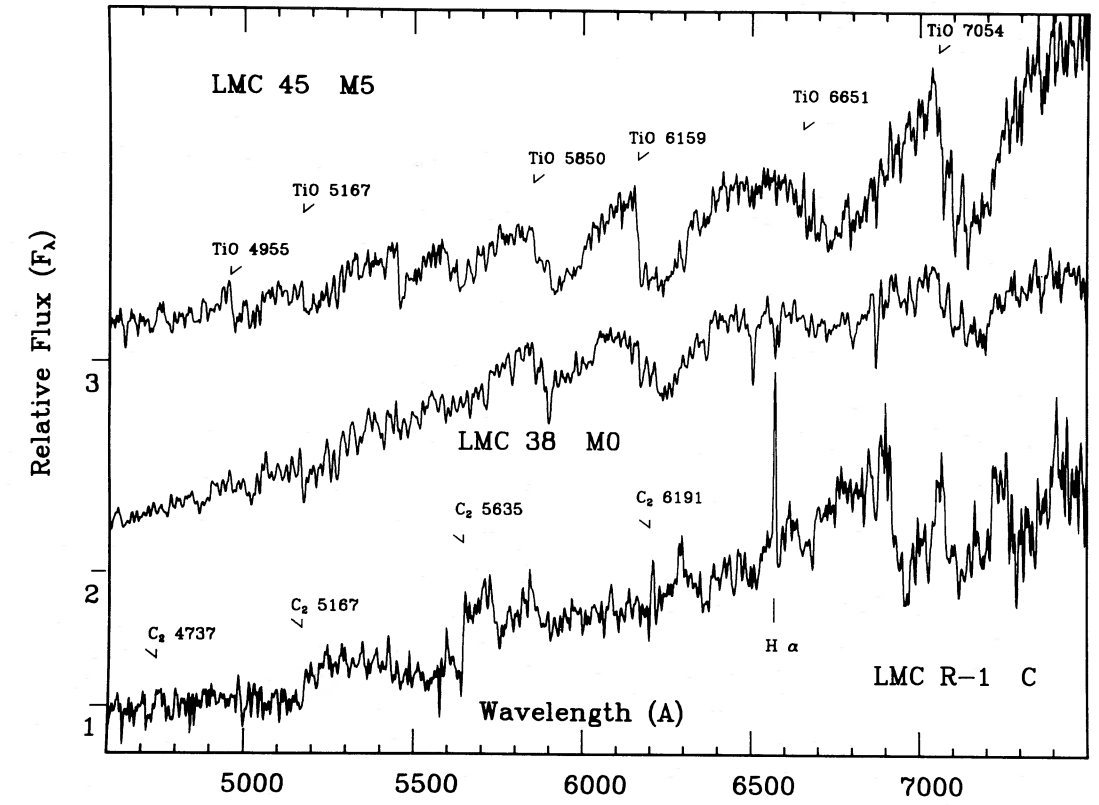

FIG. 2*a*

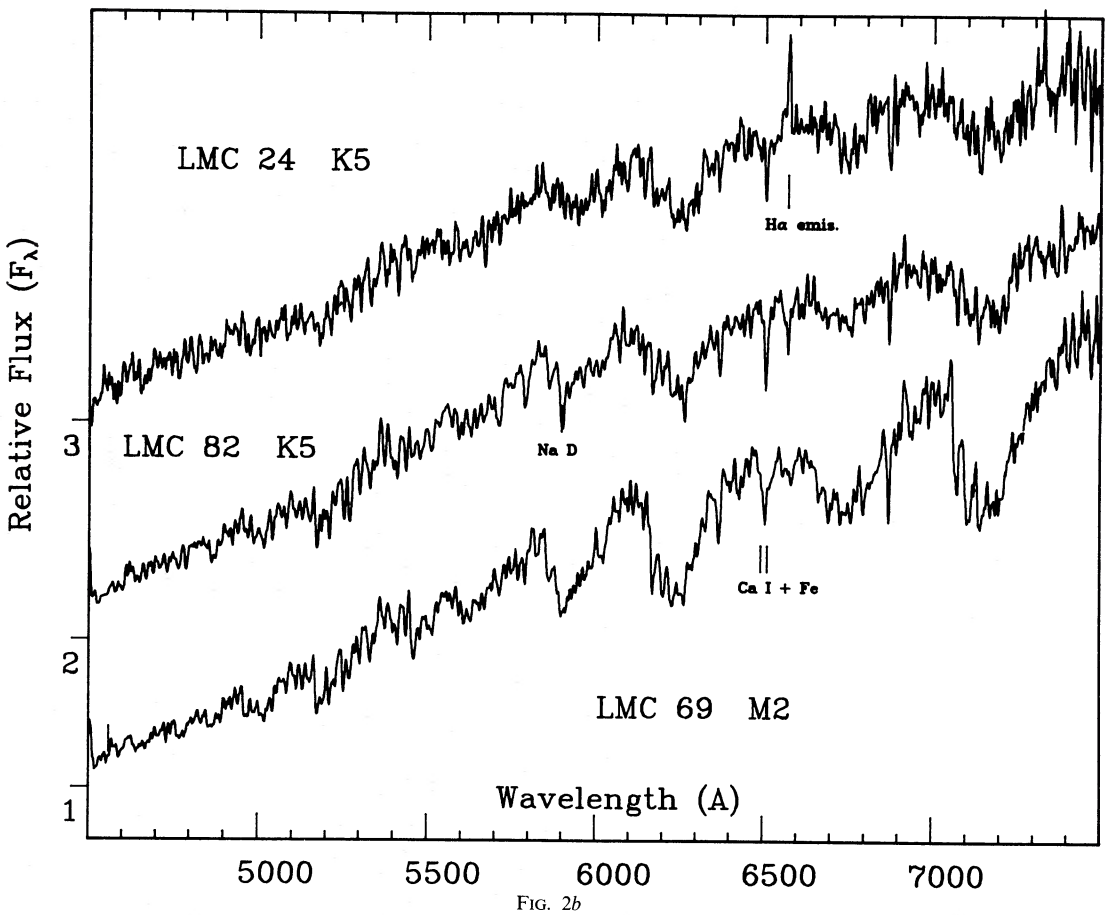

FIG. 2*b*

FIG. 2.—Spectra of selected stars from (*a–d*) the LCO and (*e, f*) AAO observations of LMC field AGB candidates. Distinctive spectroscopic features are identified and the zeropoints of the relative F_λ scale separately indicated for each star.

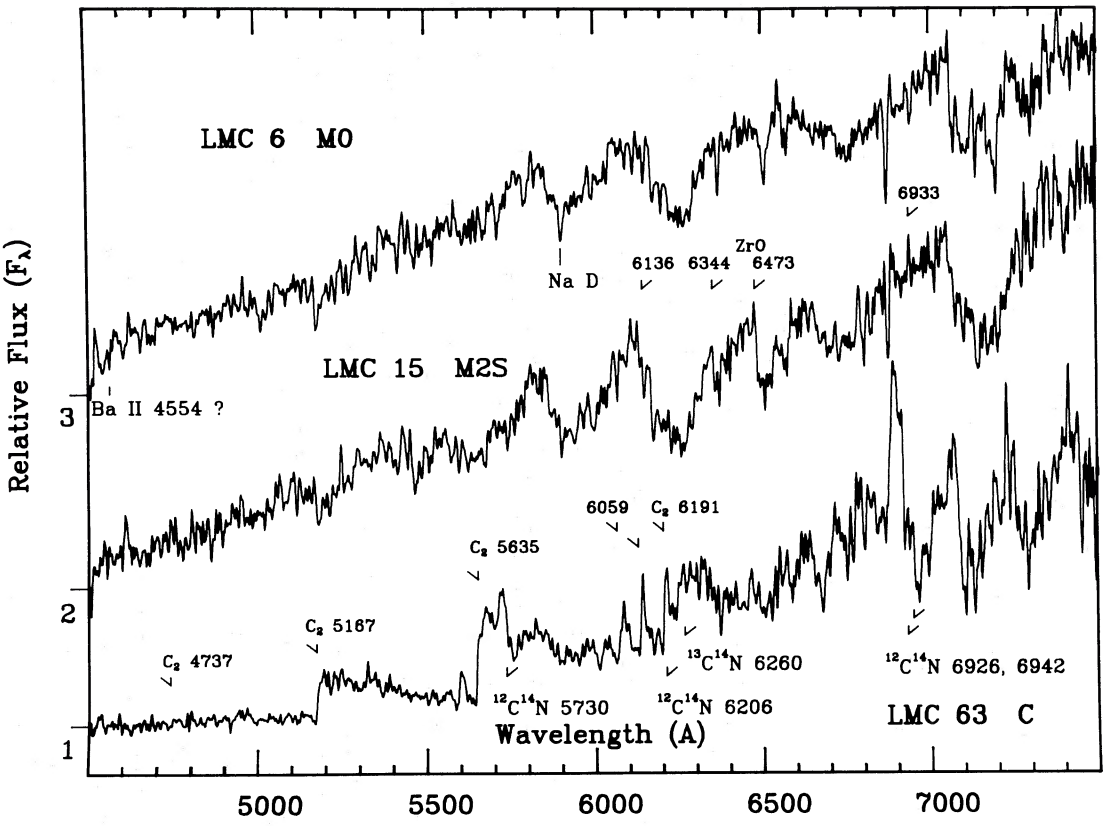

FIG. 2c

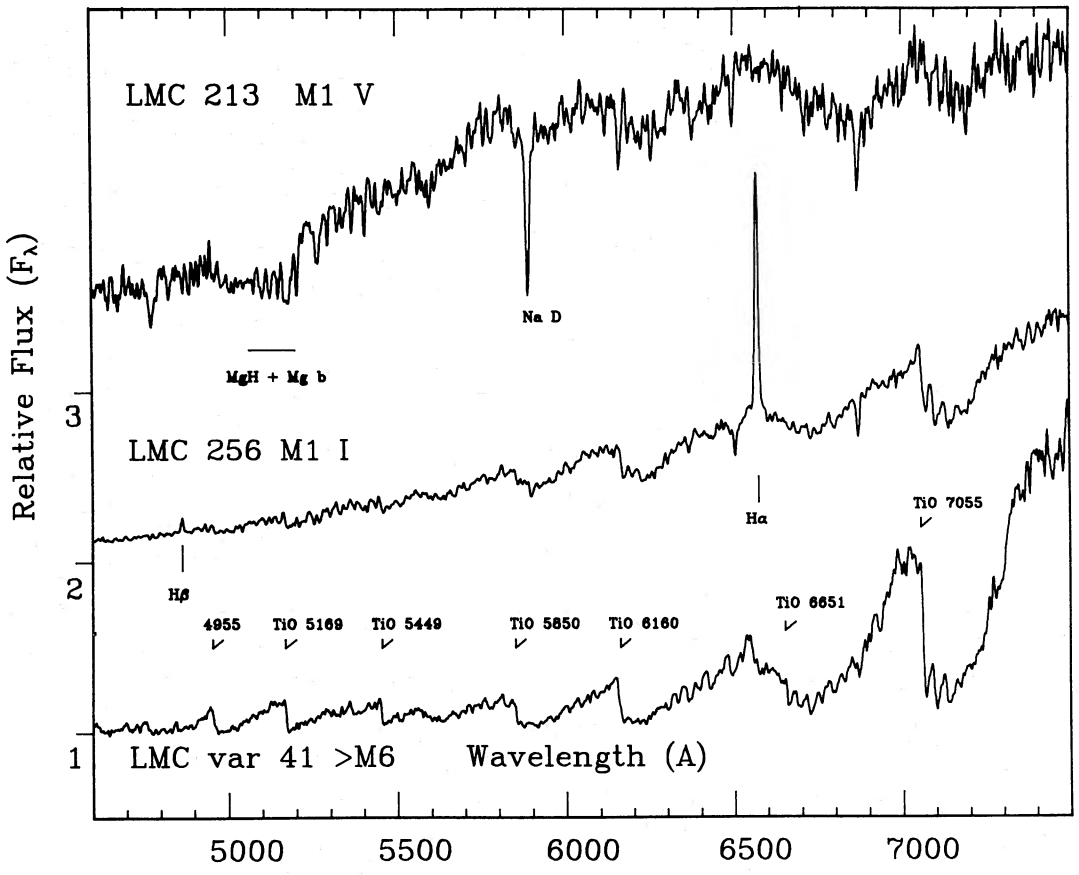

FIG. 2d

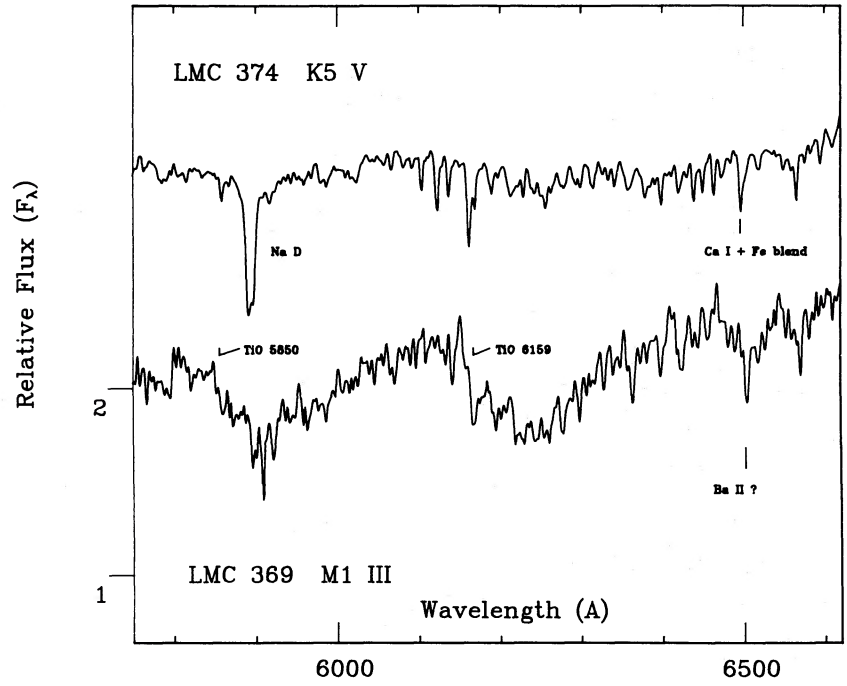

FIG. 2e

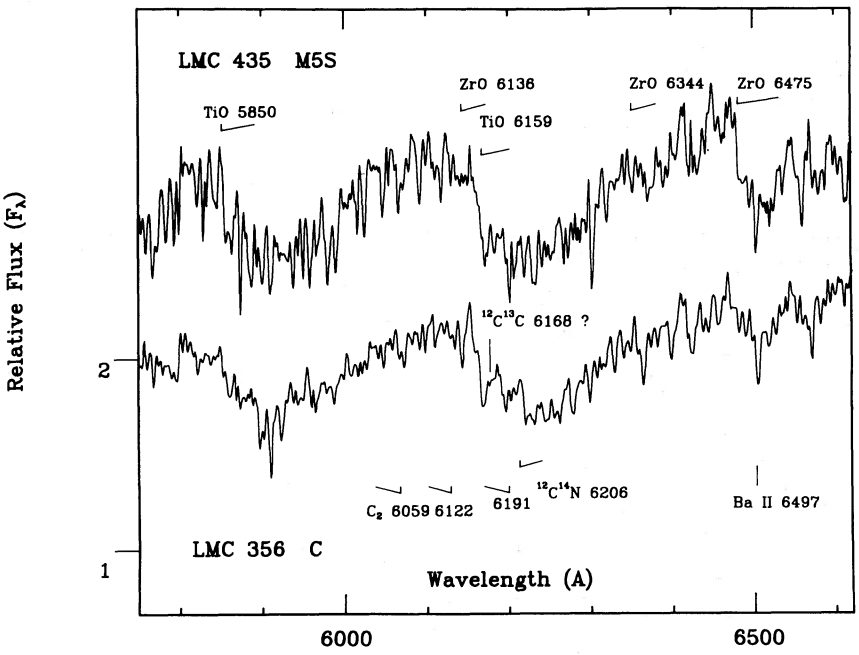

FIG. 2f

wavelengths of all indices have been correspondingly redshifted for all the confirmed LMC giants in Table 1).

The ZrO band at 6472 Å is a probable indicator of the presence of *s*-process elements in the stellar atmosphere, and the Dλ6475 index measures the strength of this band. Figure 3*c* plots this index against $V-I$ for the LMC sample. Again, most of the stars occupy a well-defined sequence, with carbon stars and a few M-type stars at larger band strengths. The latter have been classified as S stars in Table 1. TiO band strength itself is measured using both the λ6159 [γ^1(0, 0)] (Fig. 3*d*) and λ7054 [γ(0, 0)] band heads (the latter being beyond the range of the AAO spectra). From our observations of the standard stars we have derived an approximate relation between Dλ6160, the strength of the former TiO feature, and spectral type, and this has been used to derive the types quoted in Table 1. This calibration breaks down for very late type M stars—such as the LMC variables or Baades Window stars—where the "continuum" sidebands become severely cut up by TiO and VO molecular bands. Our Dλ6160 types can be calibrated against previous systems based on the Dλ7100 index (e.g.,

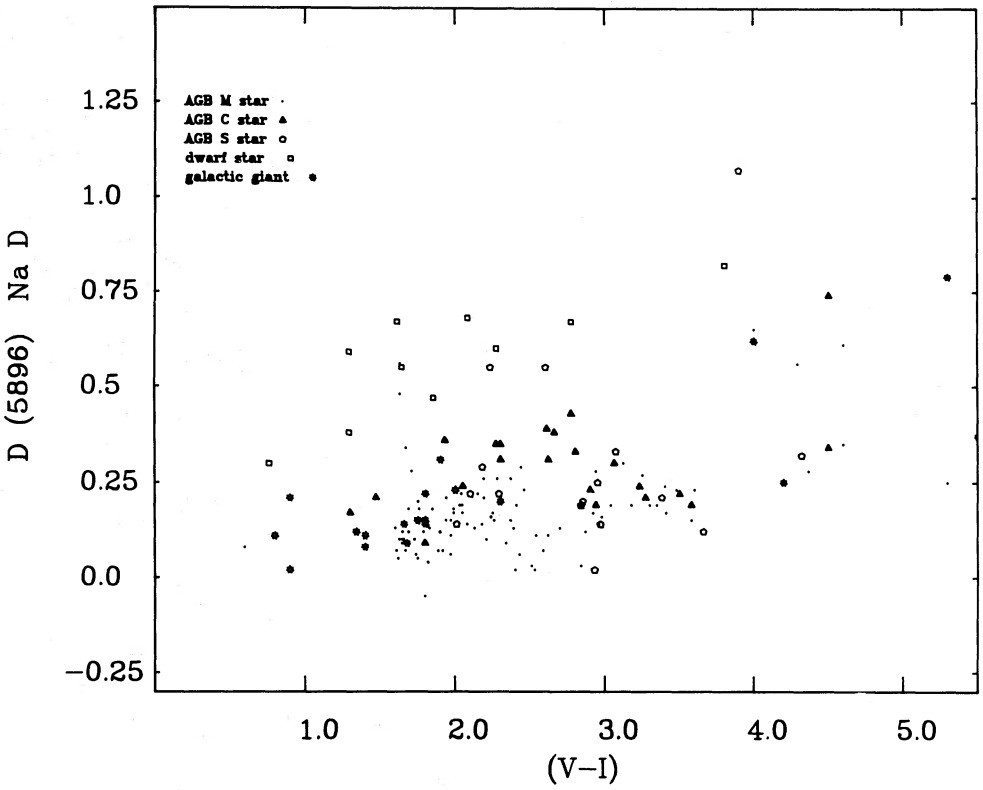

FIG. 3*a*

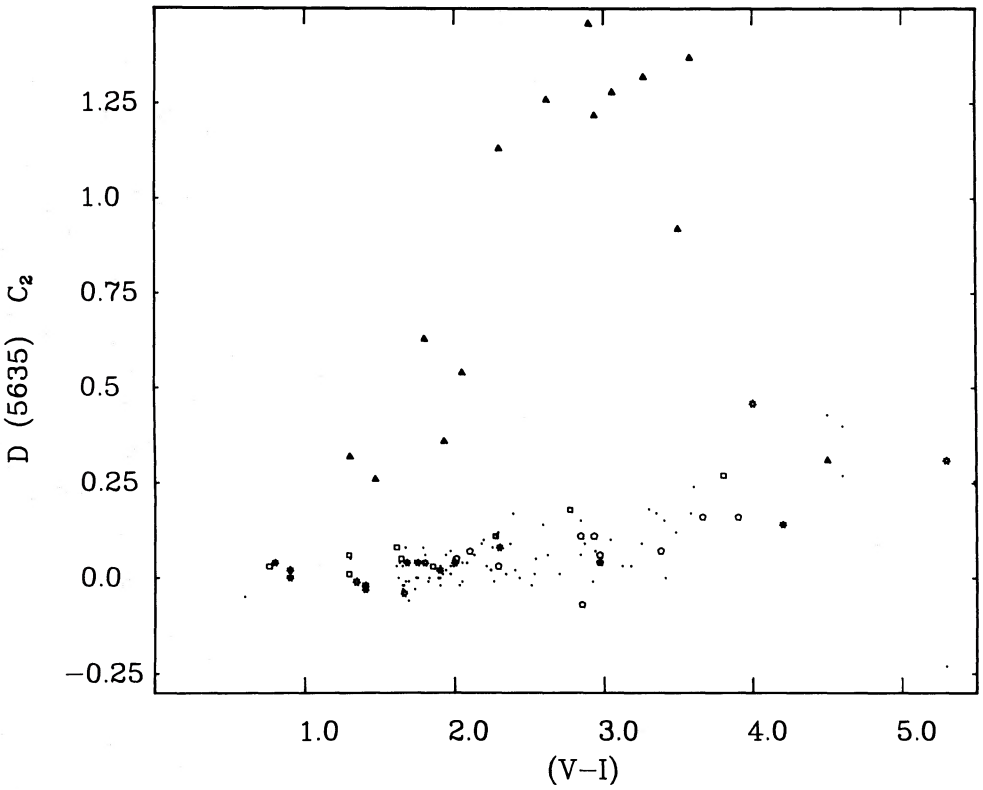

FIG. 3*b*

FIG. 3.—Narrow-band indices computed from the flux-calibrated spectroscopic data. Symbols for LMC AGB M, S, and C stars, foreground dwarfs, and galactic giants are identified in Fig. 3*a*. The individual diagrams show: (*a*) Na D line strength vs. $V-I$: dwarf/giant separation. (*b*) C_2 λ5635 vs. $V-I$: C-star feature. (*c*) ZrO λ6475 vs. $V-I$: S-star feature. (*d*) TiO λ6159 vs. $V-I$: M-star feature. (*e*) Correlation between the TiO indices Dλ6160 [$\gamma(0, 0)$ λ6159] and Dλ7100 [$\gamma(0, 0)$ λ7054]. (*f*) Calibration of the spectroscopically derived $\langle 7500-5400 \rangle$ color against $V-I$.

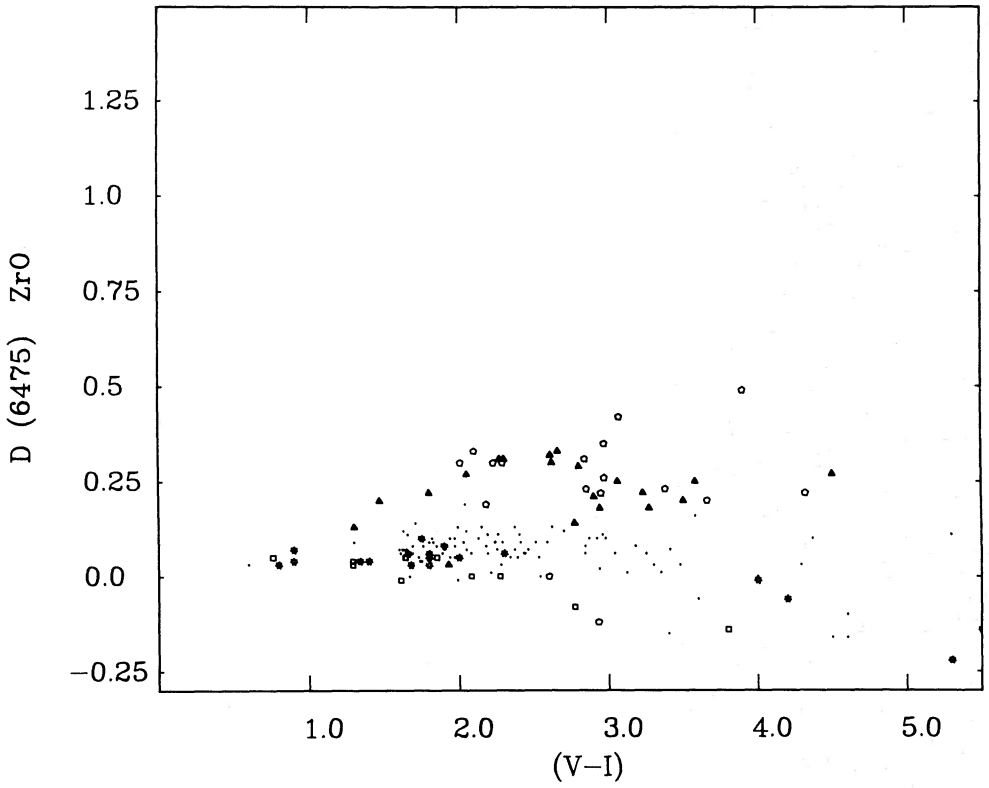

FIG. 3*c*

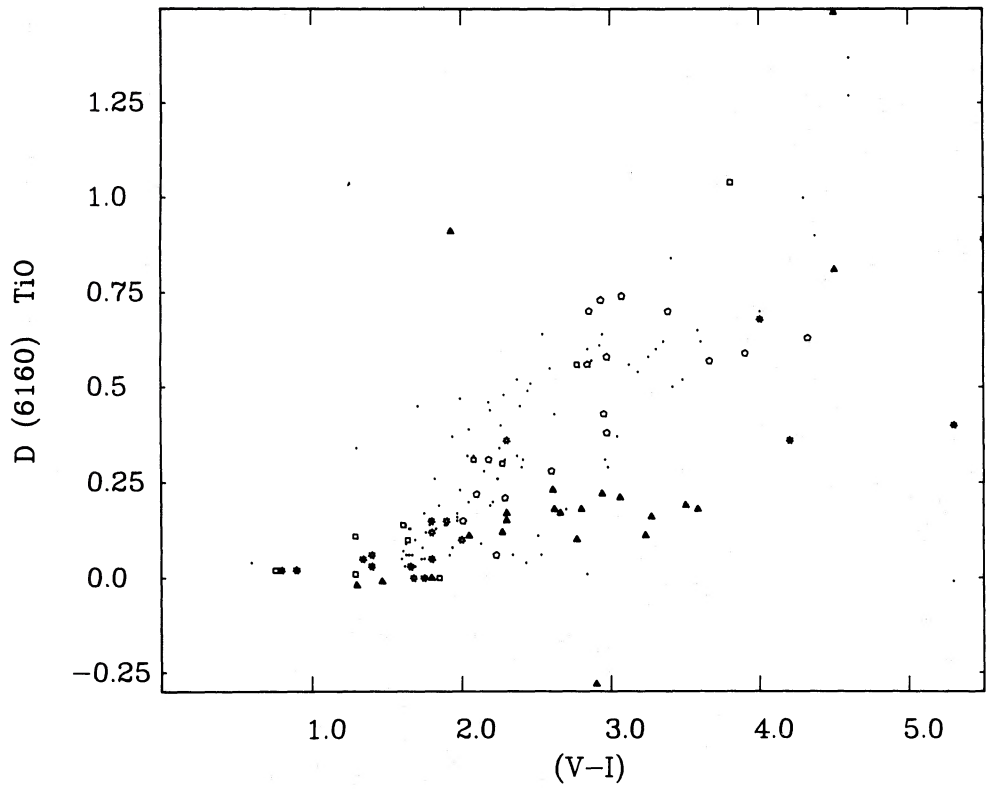

FIG. 3*d*

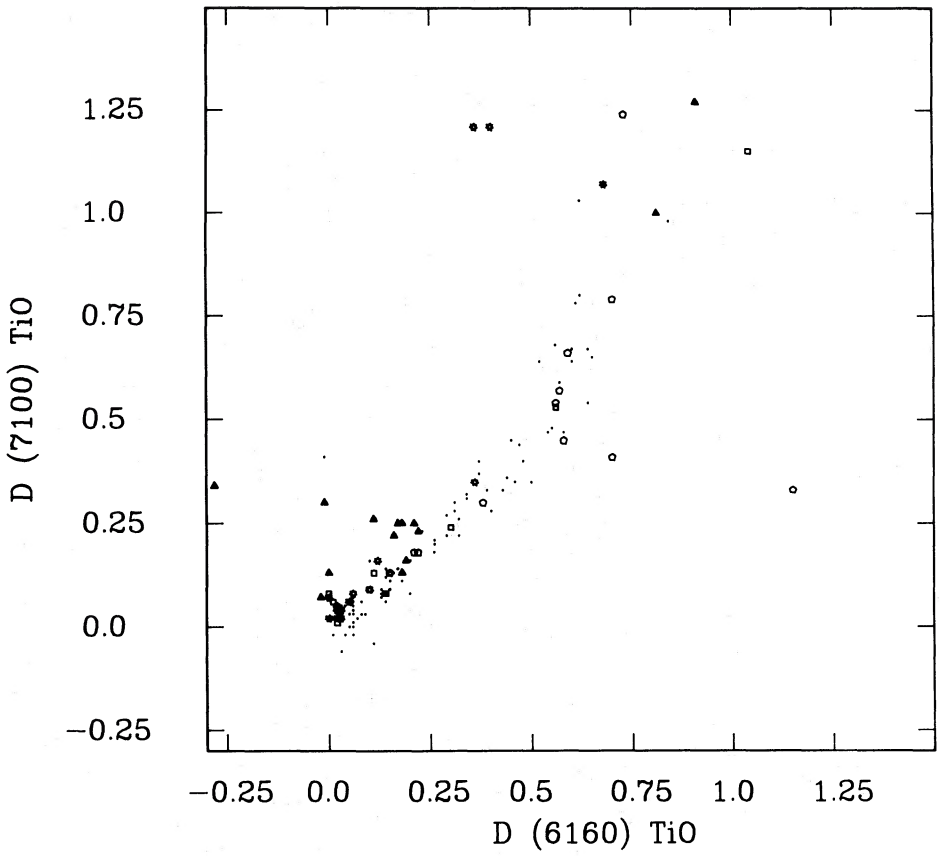

FIG. 3*e*

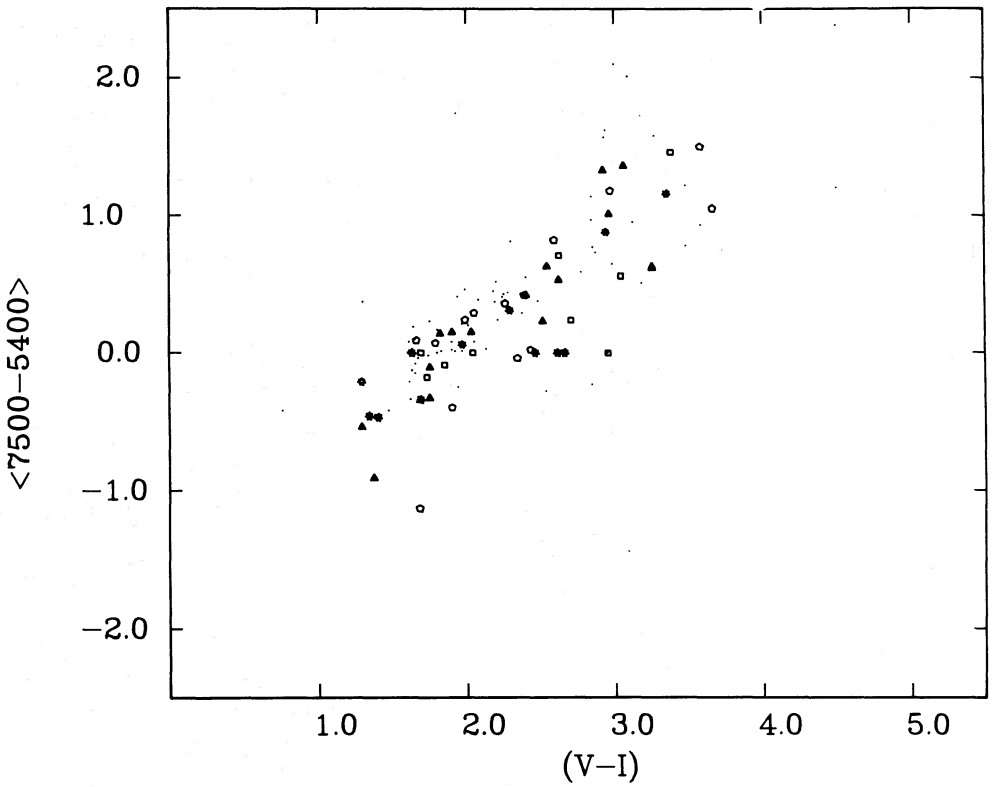

FIG. 3*f*

Mould 1983*b*) from the LCO data in Table 1. Figure 3*e* portrays this relation.

Finally, except where specifically indicated, all the spectra have at least 100 counts per channel over the wavelength range we are interested in. Hence, based on pure photon statistics, each spectrophotometric index is accurate to better than 2%–3% (depending on the bandwidth). However, the dominant uncertainties lie in the flux calibration, and repeat observations suggest that an accuracy of ± 0.03 is appropriate for the narrower band indices, and ± 0.02 for the broader Dλ6475 and Dλ7100.

b) Velocities

The spectrophotometric data provide one set of criteria for identification and classification of LMC members. As a further test, we have used standard cross-correlation methods (in this case as implemented by Keith Shortridge in the reduction package FIGARO on the Caltech VAX) to determine the relative velocities of the program stars. As standard templates we have used HD 182040 (C star), HD 198064 (MO III), and HD 195264 (M1/2 III) for the LCO data, and HD 24393 (MO) and BD $-2°891$ (M2S) for the AAO data. Except for very late types, the LCO M-star spectra, whether dwarfs or giants, cross-correlate successfully against both M-star templates. Comparing the velocities, the dispersion about the mean differences is ± 26 km s^{-1}. In the case of stars with Hα emission, the emission line velocities are also given in Table 1.

Applying similar tests to the AAO data we find a mean internal rms dispersion of 9.9 km s^{-1}, using the M stars BD $-2°891$ and HD 24093 as velocity templates. (Similarly, spectra of SA68 K giants [$\lambda\lambda$4900–5600] taken at the same dispersion and cross-correlated against a pair of radial velocity standards give rms residuals of ± 12.9 km s^{-1} about the mean difference.) Heliocentric corrections were applied in the standard manner, and the zero point of each scale was set using stars with known radial velocities. As the results in Table 1 illustrate, these external sources of calibration demonstrate that the likely accuracies of the LCO and AAO data are ± 35 km s^{-1} and ± 13 km s^{-1} respectively. While not sufficiently accurate to allow us to determine velocity structure amongst the LMC stars, these data do permit reliable identification of low-velocity foreground objects.

The mean radial velocities and dispersions within the six fields are given in Table 3, together with similar measurements for the LMC field stars and variables tabulated in the Appendix. These have been reduced to galactocentric radial velocities (col. [5]) following Feitzinger and Weiss (1979), who adopt a Galactic rotation of 250 km s^{-1} and a standard solar motion of 19.7 km s^{-1} directed toward $l = 57°$, $b = 22°$. Freeman, Illingworth, and Oemler (1983) have presented observations of LMC globulars on the same system, and Table 3 lists the radial velocities for clusters near each of our areas. Our velocities are generally consistent with these values, which supports the view that these and other LMC clusters are a disk population. The rms dispersions from the LCO observations are comparable with the external residuals, but from the AAO data we derive intrinsic velocity dispersions of 14 and 15 km s^{-1} in area F and for the miscellaneous field stars respectively. However, there are insufficient stars to test for different dispersions at different bolometric magnitudes. Further higher resolution observations of both these and similar AGB stars in the southern LMC will provide substantial insight into the kinematics and rotation of the different stellar populations.

c) Classification

Using both spectrophotometric and radial velocity criteria, 11 of the 113 stars in Table 1 are identified as foreground stars. Six of these are nearby dwarf stars, while four others are Galactic halo K giants, lying at distances of 2–5 kpc from the Sun. These results verify the assumption, based on star count models (Gilmore 1984; Bahcall and Soneira 1980), made in Paper I that dwarf star contamination is at a level of less than 10%, while Galactic giants form a similarly small proportion of the sample. The formal velocity dispersion of these four stars is 55 ± 19 km s^{-1}, inconsistent with either the spherical ($\sigma \approx 120$ km s^{-1}) or cylindrical ($\sigma \approx 95$ km s^{-1}) dynamical models of the Galactic halo discussed by Ratnatunga and Freeman (1985). While our statistics are meager, this lower velocity dispersion is more consistent with a "thick-disk" population (Gilmore and Reid 1983). Clearly, further observations are required. The 11th non–LMC star is LMC 167, a nearby G dwarf, which inadvertently crept into our program through the inevitable photometric error.

Amongst the LMC stars themselves, a number of M-type stars show weak ZrO features, although their Dλ6475 band strength falls beneath our S-star criterion. Others show a strengthening of the spectral feature near 6500 Å, a redshifted blend of Ca, Fe, and Ba II, although this is hard to distinguish from enhanced ZrO at this resolution. It would be of interest to know whether barium enhancement was a real contributor to this effect, as barium is an *s*-process element and would indicate convective dredge-up of all such elements, not merely a change in the C/O ratio (Iben and Renzini 1983). Most of the other spectroscopic features characteristic of barium stars lie shortward of the blue cutoff of the LCO spectra, but the Ba II λ4554 line is just within the range of these spectra. This may be present in a few stars (e.g., LMC 6) and is probably not present in others (LMC 38, 69), but the spectra have low signal-to-

TABLE 3

RADIAL VELOCITY OBSERVATIONS

R.A. (1)	Decl. (2)	Group (3)	$\langle \bar{V} \rangle$ (4)	$\langle V_c \rangle$ (5)	rms (6)	n (7)	Comments (8)
5^h28^m	$-64°50'$	A	317	90	± 30	14	LCO
5 30	−66 40	B	320	96	37	36	LCO, V(NGC 2004) = 85
5 20	−68 5	C	310	89	30	15	LCO, V(NGC 1885) = 62, V(NGC 1917) = 8
5 20	−66 55	D	299	77	25	3	LCO, V(NGC 1866) = 60
5 2	−66 55	E	290	73	19	11	AAO, V(NGC 1810) = 104, V(NGC 1818) = 82
5 2	−66 10	F	317	100	17	17	LCO, V(NGC 1783) = 60, V(NGC 1805) = 95
5 32	−65 5	Appendix	285	60	20	14	AAO, V(NGC 1978) = 62
...	...	variables	297	...	25	5	LCO

noise ratios at these wavelengths, and the blue region of the spectrum is crowded with other features. We intend to obtain higher resolution spectra to confirm these identifications.

We have checked the carbon stars in the sample for visibility of the ^{13}CN band at 6260 Å. This feature is seen in J stars, for which we used LMC J-4-9 as a standard (star 131 in Westerlund *et al.* 1978). There were no instances of strong 6260 Å in our sample, which suggests that envelope-burning is not effective in conversion of triple-α ^{12}C to ^{13}C in a majority of carbon stars. We have also found no case of enhanced Li λ6707 in the sample.

One other star deserves special mention, LMC 441. This has strong sodium D, initially suggesting classification as a foreground Galactic dwarf. However, the radial velocity of 272 km s^{-1} is that of an LMC star. Our observations are limited to 5750–6650 Å, but as Figure 4 shows, LMC 441 is strikingly similar to, although not as extreme as, the SC5-6 star R CMi. It is possible that the Na D strength is enhanced by neighboring CaCl absorption. LMC 441, therefore, is probably an AGB star caught during the transition from S to C—a hypothesis consistent with the bolometric magnitude of ~ -5.3. Fuller spectral coverage is needed to confirm this.

Finally, a few of the latest spectral types show VO molecular absorption near 7200 Å, but the majority of these stars are to be found among the variables with only three stars of spectral type M6 or later within our volume-complete sample. Finally, those stars with hydrogen emission features have been identified in Table 1.

IV. THE AGB LUMINOSITY FUNCTION

a) Survey Completeness

Our new observational data allow us to extend Paper I's analysis of the AGB–star luminosity function, making more accurate allowance for foreground contamination and adding the extra dimension of surface composition. Before doing so, however, we reconsider the completeness of our sample. As Paper I describes, stars redder than $V-I = 1.6$, the peak of the M92 first giant branch, are identified as AGB stars. In contrast, other surveys (Westerlund, Olander, and Heden 1981; Blanco, McCarthy, and Blanco 1980, hereafter BMB80); Blanco and McCarthy 1983, hereafter BM83) use objective prism or grism techniques. We have already discussed the Westerlund *et al.* C stars in Paper I and shown that, allowing for merged images, our data are 95% complete with respect to that survey. We now consider the deeper BMB80 survey, based on CTIO 4 m telescope grism plates of 52 fields in the LMC.

Nine of the BMB80 fields lie within our LMC (north) field (areas 8, 13, 17, 18, 19, 24, 27, 29, and 31). We have compared the spectroscopic and photometric data in three of these fields (17, 18, and 19), cross-identifying stars using the original grism plates kindly provided by Dr. V. M. Blanco. These allow a preliminary assessment of our completeness relative to BMB80. A small section of BMB80-17 overlaps with one of the exclusion zones outlined in Paper I. One C star and two of the late-type ($\geq$M6) M stars identified by BMB80 are merged images in our COSMOS data. All remaining 36 C stars and 10

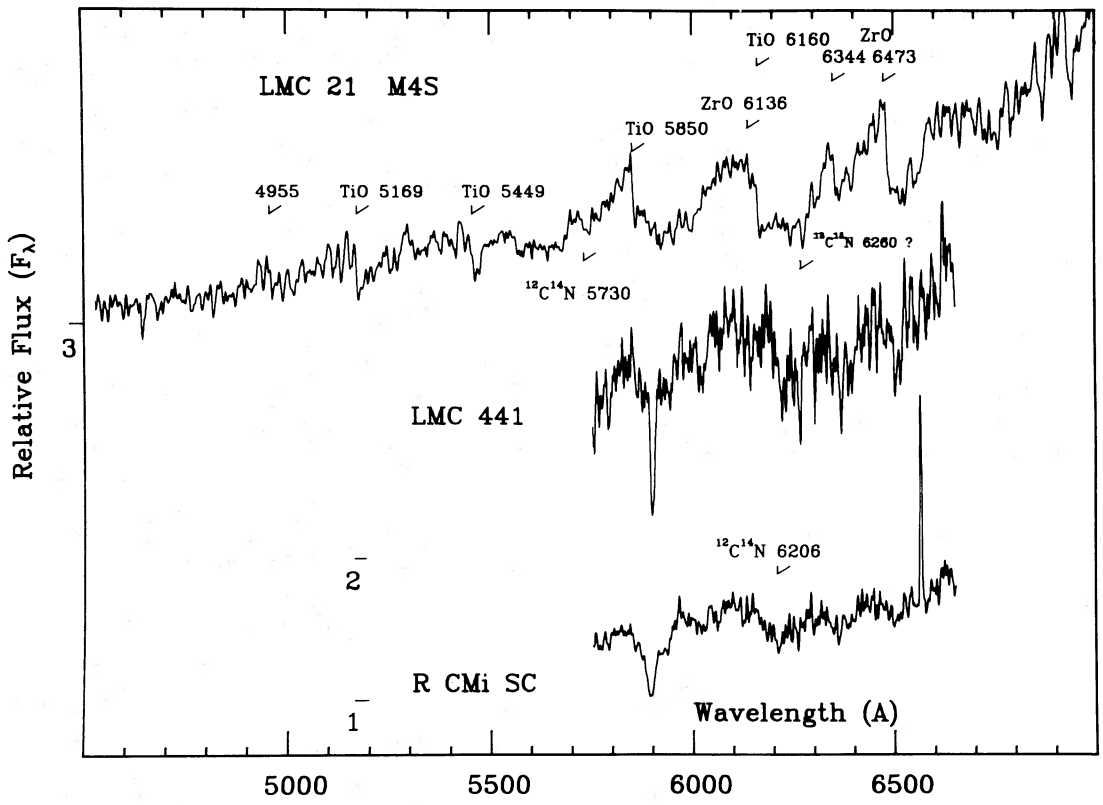

FIG. 4.—(*1*), (*2*) AAT CCD spectra of the Galactic SC star R CMi and LMC 441, a probable SC star in the LMC. (*3*) The LCO spectrum of LMC 21, possibly an S star with dredged-up ^{13}C. ^{13}C ^{14}N λ6260 is tentatively identified.

late-type M stars are included in our photometrically defined AGB sample—as indeed are all the earlier type (M4–5) M stars in BMB80. On the other hand, while the grism survey encompasses all stars with $V-I \geq 4$, at least for these areas it includes only $\sim 50\%$ of stars with colors in the range $3 \leq V-I < 4$. In addition, while the mean $V-I$ color of the M6 giants is redder than that of the M4–5 stars (3.38 as opposed to 3.19), there is a substantial overlap among the individual stellar colors. The earlier stars span $2.45 \leq V-I \leq 3.82$, while the later types cover $2.12 \leq V-I \leq 4.63$.

This comparison first shows that our data are complete with regard to the BMB80 survey. Indeed our AGB sample is more extensive, primarily because it covers earlier spectral types, but also among the redder stars. BM83 have presented extensive evidence for the completeness of the spectroscopic survey in detecting the distinctive C-star spectra. It is likely, therefore, that the "missing" stars are M giants. $V-I = 3$ is equivalent to a spectral type of M5 III (Bessell 1979). Clearly, further observations extending to all BMB80 areas in our LMC (north) field are required to test this implied incompleteness. For the present, however, we assume that the grism data are complete for C stars, while our photometric results include all AGB stars. Under these assumptions we go on to consider the C/M ratio on the upper AGB.

b) *The* C/M *Ratio on the AGB*

Using our photometry and the bolometric correction prescription given in § III, we have calculated absolute bolometric magnitudes for all C stars identified in BMB80-17, -18, and -19. The mean absolute magnitude of the sample is -4.84, and the brightest star has an M_{bol} of -5.6: properties similar to the C stars in our survey, as discussed further in § IV*c*. Moreover, only two stars of the 36 in the sample have $M_{bol} > -4$. Hence we can compare these areas with our survey areas A and B (see Fig. 5).

Table 4 shows the relative numbers of C and M (or S) stars in the five areas. As discussed in § IV*a*, the noncarbon stars in the BMB80 areas consist of our AGB candidates with $-7 < M_{bol} < -4$ minus the known carbon stars. We have also slightly modified the BMB80 areas, squaring their circles, to simplify defining each area. Finally, NGC 1866 lies in the center of BMB80-19, and to avoid including cluster AGB stars in our comparison we have excluded all red stars within 5′ of the cluster center. These alterations account for the differences between the C-star numbers given here and those in BM83.

Although our statistics are not overwhelming, there is evidence for significant variations in the C/non-C ratio from field to field. In general terms this may be correlated with the distance from the Bar, although BMB80-17, near NGC 1846, has the highest C-star content. This result disagrees with BM83's conclusion that the C/M ratio is uniform over the LMC, but note that they consider *only* the latest M stars. We have already discussed our C-star completeness, but it is worth pointing out that the surface density of C stars in fields A and B is in good agreement with the isopleths presented in BM83. Even so, with only one C star, the low value in area A could easily be due to sampling statistics, and more extensive observations are being obtained of stars in these outer regions to check this result. However, the higher density of C stars in BMB80-18, and, especially, -17 are less easily accounted for in this manner.

TABLE 4

NUMBERS OF STARS

Area	C Stars	M/S Star	C/non-C	R_5
BMB80-17	14	25	0.56	1.27
BMB80-18	16	42	0.38	1.08
BMB80-19	6	22	0.27	1.56
A	1	12	0.08	0.63
B	5	27	0.19	1.88

Iben and Renzini (1983) have outlined three factors which may conspire to change the C/M ratio on the AGB. Two are metallicity-dependent; decreasing metallicity both increases the fraction of C stars formed and moves M stars to higher temperatures at a given luminosity. Hence in a spectral type (or color)–defined sample, C/M increases with decreasing metallicity. The third factor is a dependence on age: in an old ($\sim 10^{10}$ yr) stellar population, the stars evolving on the AGB lose their envelopes to mass loss before the critical core mass for thermal pulsing is attained.

Abundance variations are probably responsible for the increasing trend in C/M moving from the Galactic bulge through the disk and LMC to the SMC. However, our result implies a metallicity gradient in the LMC such that the Bar is less enriched than the outer regions. From observations of H II regions, Pagel *et al.* (1978) find marginal evidence for a slight gradient in the opposite sense. In a qualitative sense, it is difficult to envisage a palatable mechanism that selectively enhances the metallicity in regions well away from the main site of star formation. Hence we think it unlikely that abundance variations are responsible for the low C/non-C star ratios in the outer fields. Differing star formation histories, on the other hand, appear to be a plausible way of accounting for these data. In the following section we apply the disparate luminosity functions of the various areas to a more detailed examination of this hypothesis.

c) *The AGB Luminosity Function(s)*

We have derived luminosity functions for each of the six areas A–F, omitting non-LMC stars, and the results are displayed in Figure 5. It is apparent that our data represent two types of luminosity function: type A, found in the low star density areas A, D, and E, characterized by an almost total absence of the intrinsically most luminous ($M_{bol} < -6$) stars; and type B, in areas B, C, and F, with almost equal proportions of high and low luminosity stars, as well as a number of stars brighter than the upper AGB limit of $M_{bol} \sim -7$. Brighter than $M_{bol} = -5$ we have averaged data over the three fields in each subset, but at fainter magnitudes we only have observations in fields A and B. Hence we have effectively given these stars triple weight in the diagram. Future observations will extend the luminosity functions in the other areas to check our results. Note that with our revised M_{bol} calibration a number of stars fall beneath the M_{bol} limit in each field, and these have been excluded from the composite functions.

Figure 5 illustrates the absolute magnitude distribution of the different spectral types in the type A and B fields. To a limited extent we can do the same for the BMB80 fields, making the same assumptions as outlined in § IV*b*, and these functions are also shown in Figure 5. This ensemble of specific luminosity functions poses two problems.

In each field, C stars lie in the range $-4 < M_{bol} < -5.5$, as originally demonstrated in BMB80. Furthermore, our data show that S stars occupy the same range of luminosity in the

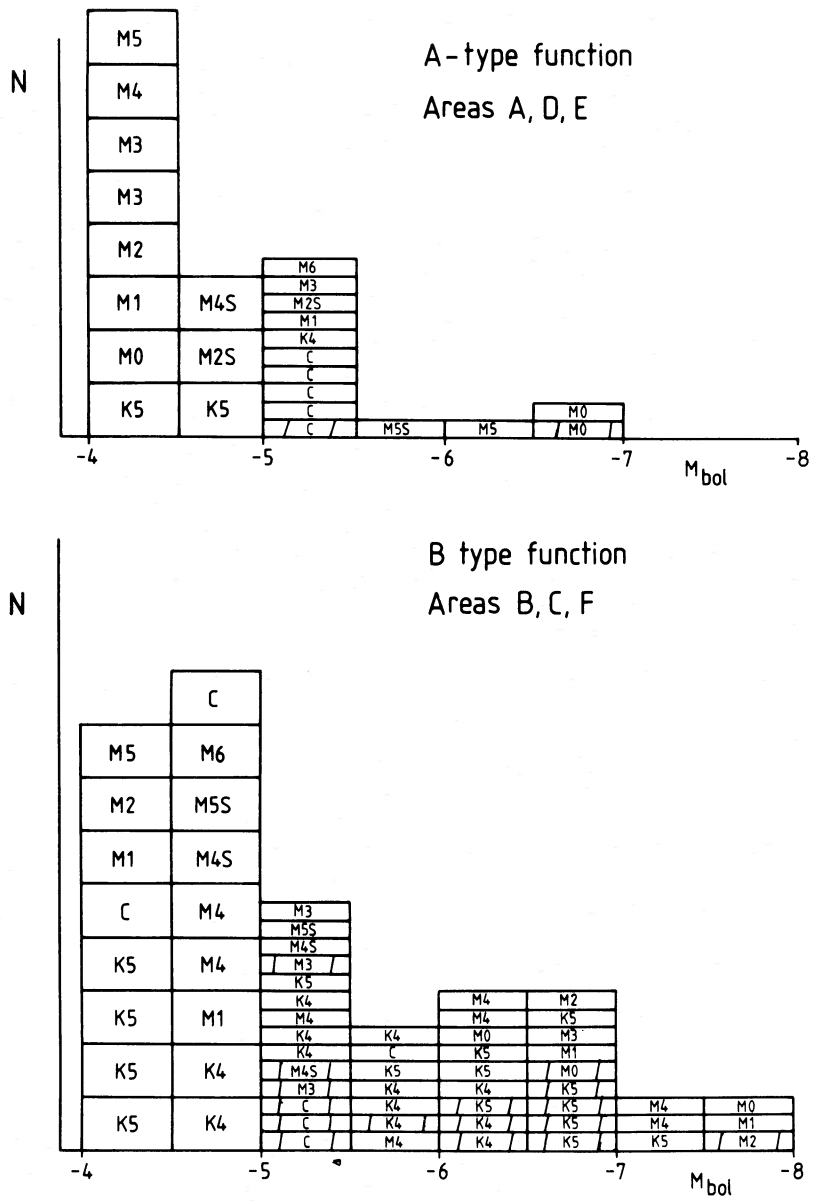

FIG. 5.—The specific luminosity functions for type A and type B areas. As described in the text, our observations extend to $M_{bol} = -4$ only in areas A and B themselves, and the luminosity functions brighter than $M_{bol} = -5$ represent linear combinations of the areas indicated. The individual contributions of areas A (two stars) and B (16 stars) to the more luminous stars are indicated.

main, although note LMC 435 (our Appendix 1 and Fig. 2).[2] Thus, while the onset of atmospheric contamination by *s*-process elements is broadly in agreement with theoretical predictions, there remains a conspicuous absence of stars clearly identifiable as more luminous AGB stars. Instead, the majority of stars with $M_{bol} < -6$ are late K-, early M-type, which display no evidence of having undergone thermal pulses and subsequent dredge-up. That is one problem; the second we have already alluded to: the variation in C/non-C ratio among the five fields of Table 4.

Considering first the $M_{bol} < -6$ stars, we notice that the three type B areas lie close to well-known H II regions and also enclose more luminous short-lived K and M supergiants. This inevitably suggests that the "luminous AGB" stars are predominantly young stars, more massive than $\sim 10\,M_{\odot}$, and on the first ascent of the red giant/supergiant branch. Against this, Wood, Bessell, and Fox (1981) have shown that LMC variables exist with luminosities in this range and pulsational masses consistent with lower mass, AGB stars. However, we argue that these are a minority constituent of the LMC field we have surveyed.

We can test our hypothesis over the whole LMC (north) field by using the distribution of luminous red stars to partition the AGB candidates. Theory states that stars with M_{bol} in the range $(-7, -8)$ cannot be on the AGB, since the core mass required violates the Chandrasekhar limit. A few will be foreground dwarfs or giants, but the majority are LMC supergiants. Dividing our field into 100 equal-opportunity boxes, we have compiled separate luminosity functions from AGB stars

[2] Indeed there is a surprising proliferation of stars showing S-type features, given that these stars require a C/O ratio close to 1.

TABLE 5

HARVARD LONG-PERIOD VARIABLES

Star	α (1950.0)	δ (1950.0)	$\langle V \rangle$	$\langle V-I \rangle$	σ_I	M_{bol}
HV 1001	$5^h35^m22^s.7$	−67°45′43″	15.55	5.05	0.28	∼−8.5
HV 2360[a]	5 15 34.7	−66 8 12	18.23	5.61	0.98	−7.3[a]
HV 2379	5 15 6.4	−67 59 18	16.89	3.24	0.14	−4.8
HV 2446	5 20 7.5	−67 37 37	17.35	4.07	1.42	−5.7
HV 2555	5 28 14.3	−66 34 0	15.20	2.23	0.08	−5.2
HV 2575	5 29 8.3	−67 47 16	16.85	4.05	0.13	−6.3
HV 2586[a]	5 29 36.7	−66 57 43	12.24	1.79	0.14	−7.6[a]
HV 5854[a]	5 28 17.6	−67 1 11	13.45	2.94	0.08	−8.0[a]
HV 6103	5 15 34.7	−66 8 12	18.73	5.61	0.98	−7.0
HV 12227	5 3 43.1	−66 20 1	15.63	1.74	1.34	−4.2
HV 12439	5 33 48.7	−68 7 54	16.89	2.94	0.98	−4.5

[a] Within Paper I exclusion zones.

in boxes which enclose supergiants (53) and from the rest of the field. The relevant functions are shown in Figure 6, where it is clear that the latter, supergiantless region function is similar to the type A function. The absence of $M_{bol} \approx -6.5$ stars clearly indicates that they are spatially correlated with the supergiants, supporting our hypothesis that they are mainly drawn from the same young stellar population.

The solution to the second problem is less clear cut. We have already dismissed abundance variations as a physically plausible mechanism, leaving the star formation history alternative. An older stellar population, with less massive stars in the AGB phase, will have a general deficiency of upper AGB stars, and hence C stars (see Fig. 6). Does the stubby type A function indicate an older predominant population in this area? We can test for this in a crudely quantitative way by setting in ratio the number of stars in the bolometric range (−4.5, −5.5) and (−4, −4.5) for each area, and this ratio is tabulated as R_5 in Table 4. Area A does have a low value, consistent with older, lower mass stars, but the samples again are sparse. In terms of the star formation history, we interpret this as a reduced birthrate in the the outer LMC over the last ∼3 Gyr although the solitary $M_{bol} \approx -6.7$ star does indicate a continuing dribble.

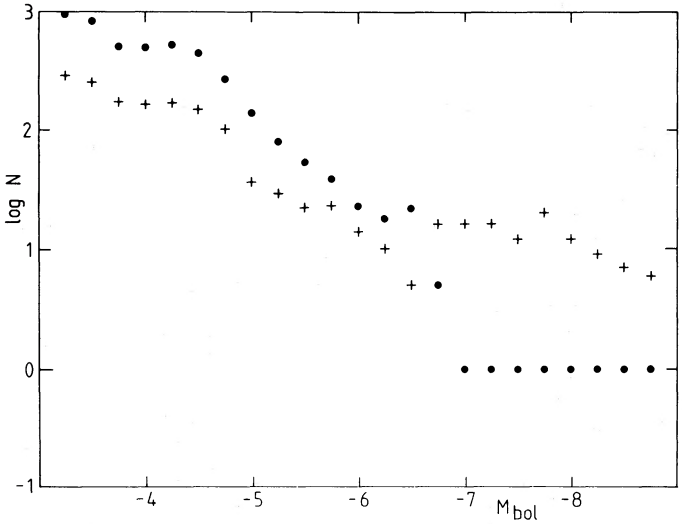

FIG. 6.—Photometric luminosity functions for AGB candidates in regions of the field (*a*) populated by supergiants ($M_{bol} < -7$) (*plusses*) and (*b*) unpopulated by supergiants (*filled circles*). These functions are derived by dividing the field into 100 boxes, 53 of which contribute to (*a*).

Near the Bar, on the other hand, star formation has been maintained at a higher level. Given the present distribution of gas in the LMC, this is not a radical suggestion. However, with more detailed and extensive observations it should be possible to refine considerably this assessment. In the following section, however, we shall ignore these possible spatial variations and conduct a more quantitative analysis of the field as a whole.

V. AGB EVOLUTION AND STAR FORMATION HISTORY

Paper I described the calculation of a simple model for the measured luminosity function, based on an assumed history of the star formation rate (SFR), the flat luminosity function for AGB stars of a given mass, and an assumed initial mass function. We can now introduce a number of improvements to that simple model.

1. A smooth curve is drawn through the data of Aaronson and Mould (1984) to represent the empirical relation between AGB tip luminosity and age. The new relation is shown in Figure 7, where it is seen to truncate the AGB at lower luminosities than the previous theoretical relation. We allow it to join the curve representing the start of thermal pulses (Iben and Renzini 1983, Fig. 7) at approximately 10^8 yr. The additional mass loss that we postulate in this way could physically occur either in a steady wind driven throughout the 10^6 yr time scale for AGB evolution, or as a 10^4 yr "superwind" (Renzini and Voli 1981; Baud 1982), preceding planetary nebula formation.

2. An explicit treatment of the early-AGB phase, which precedes the onset of thermal pulses, has been included. During this phase we substitute

$$dt = d \log L 10^{-1.92}(2/M_i)^{3.6} \text{ Gyr}$$

for equation (3) of Paper I. In this equation (Iben and Renzini 1983), M_i is the main-sequence stellar mass (or 2 $M_\odot$, whichever is larger).

3. We have increased the size of the interpulse dip in luminosity to something more appropriate to low-mass stars. Specifically, we assume

$$\Delta M_{bol} = 0.25, 20\% \text{ of the time};$$
$$= 0.50, 10\% \text{ of the time};$$
$$= 1.00, 10\% \text{ of the time}.$$

This is a better approximation to Iben and Renzini's (1983) Figure 4.

4. AGB stars of large initial mass (up to 9 $M_\odot$) have been

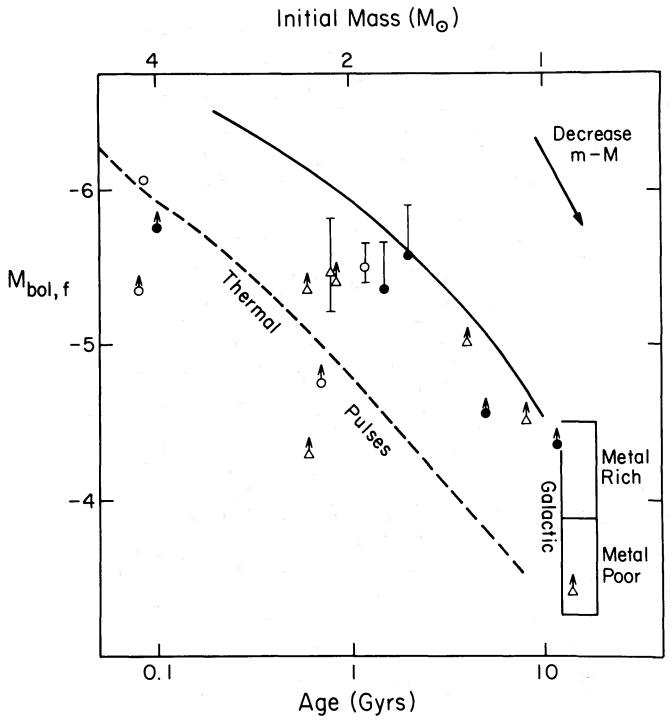

FIG.—7.—The AGB-tip luminosity/age relation from Magellanic Cloud clusters.

included explicitly. The only remaining external correction required to the model is for core helium–burning (CHB) stars of 5–15 $M_\odot$.

With this model let us consider the type A luminosity function under the standard assumption of a constant star formation rate. As shown in Figure 8, a model of age 4 Gyr—i.e., continuous star formation over the last 4 Gyr–produces quite a good fit to the observed distribution. The first of the modifications described above has effectively prevented the more common low-mass AGB stars from reaching higher luminosities. The model predicts that an increasing percentage of stars have undergone thermal pulses with increasing luminosity. This is an upper limit on the number of observed carbon and S stars, since the younger, more metal-rich members of the population will presumably require more dredge-up to neutralize their preexisting oxygen. Note that the 4 Gyr old model may seem a better fit to the data than a 16 Gyr old model. But beware of possible incompleteness in the first bin of the luminosity function. As a correction to the model, we estimate eight CHB stars exist in the type A portion of the field, mostly between -4.5 and -6 in M_{bol}. This estimate is based on the lifetimes of red giants in Becker's (1981) models.

The type B luminosity function, however, contains a tail of bright stars ($M_{bol} < -5.5$), not provided in the constant SFR model. If our empirical AGB tip relation is correct, these must be stars more massive than 5 $M_\odot$. Alternatively, one might suppose these stars represented the tail of a significant dispersion in mass loss rates existing on the AGB. The dearth of S and C stars among their number, however, strongly argues against this hypothesis.

If stars brighter than -6 are more massive than 5 $M_\odot$, they must have formed less than 10^8 yr ago in a recent burst of star formation. When we add such a feature to the model (a factor of 10 increase in SFR 10^8 yr ago), we see only a modest extension of the AGB luminosity function (Fig. 8), but an increase in the number of CHB stars predicted to 90 stars, more than enough to make up the missing bright component. It is hard to be specific about the luminosity distribution of these CHB stars, except to note that significant numbers of stars between 10 and 15 $M_\odot$ are required to extend the luminosity function tail all the way to $M_{bol} = -7$. But it is clear that these stars are expected to be mostly CHB stars (with giant branch lifetimes of 4×10^5 yr at 11 $M_\odot$) rather than AGB stars with lifetimes less than 10^5 yr per magnitude for $M_i > 6\ M_\odot$.

The total mass in the recent burst is large—nominally, 20% of the overall mass now in stars. But this fraction is not strongly constrained by the model. A two-burst model for the AGB luminosity function has been suggested by Frogel and Blanco (1983). Such a star formation history could also probably be made consistent with the present observations.

VI. DISCUSSION

Our survey confirms the overall scarcity of high-luminosity C stars that was originally discovered by BMB80. However, we have also suggested that there is a gradient in the C/non-C star ratio such that there are more C stars near the Bar, a feature we have ascribed to more sporadic star formation in the outer regions of the LMC and a correspondingly older population. This hypothesis, that older, less massive AGB stars are less likely to dredge up sufficient *s*-process material to become C stars, can be tested to some extent using observations of AGB stars in Magellanic clusters of known age. Table 6 lists C/non-C ratios for 13 SMC and LMC clusters with ages greater than 0.5 Gyr. The data are taken from Mould and Aaronson (1979, 1982) and Aaronson and Mould (1982, 1984). We include all stars with $M_{bol} < -4$, and in constructing C/non-C ratios we have assumed that all stars identified as C-type from *JHK* photometry are indeed carbon stars.

Clearly, both the small number of clusters, especially with ages ≥ 2 Gyr, and the paucity of stars in some clusters, notably NGC 1868 and Lindsay 113, limit the power of this test. The SMC clusters have, on the whole, a higher C/non-C ratio than both our fields and the LMC clusters, but Blanco and McCarthy (1983) find this to be true of the SMC in general. As noted above, this is most likely due to the lower metal abun-

TABLE 6

CLUSTER PARAMETERS

Cluster	Age (Gyr)	N_c	N_{total}	C/non-C
SMC Clusters				
NGC 152	0.8	4	7	1.33
NGC 419	1.2	15	3	5.0
Lindsay 113	4	1	1	...
Kron 3	5	3	4	3.0
Lindsay 1	8	1	3	0.5
NGC 121	11.5	0	2	0.0
LMC Clusters				
NGC 2162	0.6	0	2	0
NGC 2190	0.6	2	3	1.5
NGC 1868	0.7	0	1	0
NGC 2209	0.8	2	2	...
NGC 2213	1.5	3	5	1.5
NGC 1978	2	5	8	1.67
NGC 2257	14	0	3	0

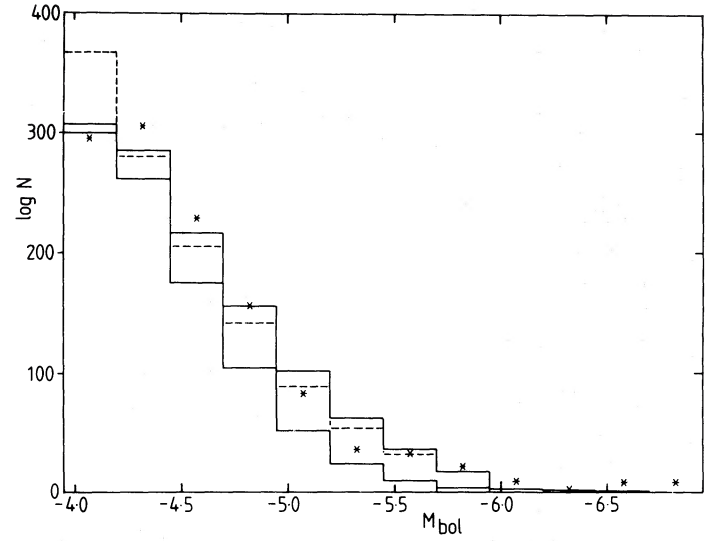

FIG. 8*a*

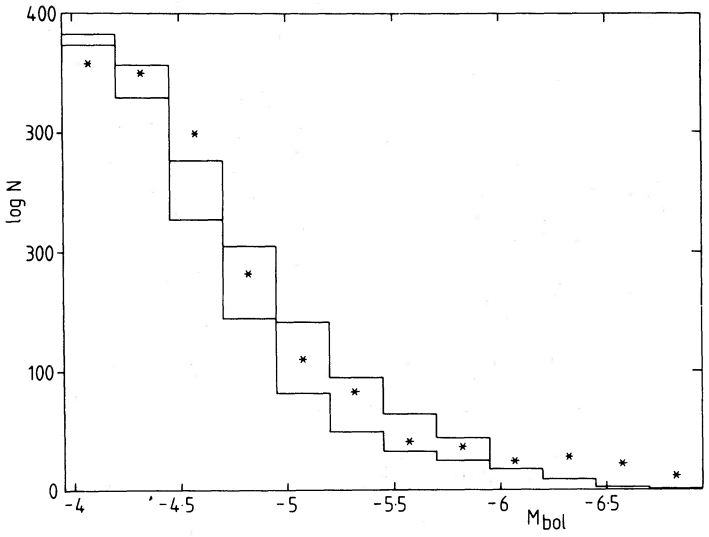

FIG. 8*b*

FIG. 8.—Star formation model luminosity functions fitted to the observed type A and type B luminosity functions. The observed luminosity functions are represented by asterisks in both diagrams. (*a*) The dashed line represents the predicted luminosity function for a model with continuous star formation over the past 16 Gyr; the upper solid line presents the model predictions for continuous star formation over the past 4 Gyr; the lower solid line represents the fraction of stars which have not undergone thermal pulses. (*b*) The lower solid line represents the fraction of stars which have not undergone thermal pulses; the upper histogram is for a model with 4 Gyr continuous star formation together with a 10^8 yr old burst.

dance in the SMC. The LMC clusters alone are too few in number and too restricted in age to illuminate this question. Determining the age of additional Magellanic clusters may afford clarification, although there may be simply too few clusters old enough to define any firm conclusions.

Considering the complete AGB sample, the simple model which fits the current observations consists of a smoothly distributed population of stars with ages up to (and possibly beyond) a few gigayears, together with a patchy young population from a recent burst of star formation. Using the star clusters of the LMC as a guide (Aaronson and Mould 1984), we would expect the portion of the old population between approximately 0.8 and 8 Gyr in age to produce carbon and S stars in the luminosity range $(-4.5, -5.5)$ in $M_{\rm bol}$. This expectation is borne out in our observed luminosity functions. The young population, in the areas where it is seen, exhibits mostly early M-type spectra, which is consistent with the longer lifetimes of CHB stars for $M > 6\ M_\odot$ and $M_{\rm bol}$ within $(-7, -6)$.

This is an internally consistent model, but what are we to make of the AGB Mira variables of Wood, Bessell, and Fox (1983) in this scenario? These stars appear to populate the full extent of the upper AGB from -4 to -7 in $M_{\rm bol}$. In Payne-Gaposhkin's (1971) Table 8, however, there are only 11 long-period variables within our field, three of which (HV 2360, 2586, 5854) lie within the exclusion zones defined in Paper I. Data from our measurements on all these stars are given in Table 5. (A twelfth one, HV 2934, lies $\sim 2'$ north of our northern declination limit, but this is the foreground, Galactic Mira variable U Dor). Of the eight variables contributing to the Paper I AGB luminosity function, only two lie in the range

$-6 > M_{bol} > -7$, 1.5% of all stars brighter than -6 in Paper I. Note also that all three variables within the exclusion zone (Shapley constellation III) have bolometric magnitudes above the AGB limit, suggesting all are supergiants.

The Payne-Gaposhkin results are supported by a more extensive variability survey currently in progress in this field (Glass and Reid 1985). The preliminary results, based on the plate material of Paper I, extend the red variable sample to 40 stars. Of these, only four have bolometric magnitudes in the range $(-7, -6)$, and all have pulsational properties more consistent with higher mass supergiants (Glass and Reid, Figs. 5 and 7). Indeed, there are no AGB stars brighter than $M_{bol} \approx -5.5$ in this sample. This contrasts with the smoother distribution found by Wood, Bessell, and Fox (1981) and, to a lesser extent, by Wood, Bessell, and Paltoglou (1985). Both the MSSSO surveys cover areas in or near the Bar, and it is possible that their results, with a higher frequency of massive intermediate-age stars, are related to the variations in the star formation history postulated in § IV*c*.

We tentatively conclude from this discussion that in the LMC (north) field AGB stars represent only a small fraction of the LMC red giant sample in this high-luminosity range. Probably this fraction consists of the most massive AGB stars (3–9 $M_{\odot}$ from the pulsational masses of Wood, Bessell, and Fox). The S star LMC 435 is the one clear-cut example in our survey, and we need to enlarge our spectroscopic sample to verify this conclusion. These luminous stars, rare though they may be, would repay closer spectroscopic attention at high resolution, since high-mass AGB stars are the favored site for the operation of the elusive envelope burning process. To make our sample truly complete at high luminosities, we also need to extend our study to the more crowded regions which were excised in Paper I. Plates of high spatial resolution will permit this to be done.

VII. CONCLUSIONS

We have obtained spectra of several area-complete samples of photometrically identified asymptotic giant branch stars in the northern LMC. Constructing luminosity functions from these samples, we find that the data are well represented by a majority population of intermediate-mass AGB stars, the result of continuous star formation over the last 3–4 Gyr or more, augmented in selected areas by younger, higher mass red giant and supergiant stars. The latter stars are the product of bursts of star formation within the last 10^8 yr. Star formation has probably been more sporadic in the outer regions, ~ 5 kpc from the Bar. Most of the stars with bolometric magnitudes between -5 and -5.5, and a smaller proportion with $-4.5 > M_{bol} > -5$, show evidence for dredge-up of *s*-process elements, although relatively few are carbon stars. We have found no evidence, however, to indicate that envelope burning is occurring in any of these stars or in our more extended sample, which reaches $M_{bol} = -7$. Future observations will extend our survey both to more crowded regions where star formation is currently in progress, and to higher spectral resolution, permitting more stringent tests of theories of nucleosynthesis and dredge-up on the asymptotic giant branch.

APPENDIX
OTHER LMC STARS AND STANDARD STARS

STAR	RA (1950)	Dec	V	V-I	Na D	D(6180) TiO	D(6475) ZrO	D(5635) C2	D(7100) TiO	Sp	M(bol)	Vel	Remarks
LMC 429	5 35 56.8	-65 18 55	16.55	3.07	0.29	0.74	0.42			M6S	-4.9	289	
LMC 430	5 35 42.2	-65 10 55	16.00	2.77	0.51	0.10	0.14			C	-5.3	292:	
LMC 431	5 35 40.6	-65 9 1	16.63	3.23	0.28	0.11	0.22			C	-5.4	266:	
LMC 432	5 35 1.7	-64 49 5	15.56	2.30	0.34	0.15	0.31			C	-4.9	281:	
LMC 433	5 35 1.3	-65 6 39	15.66	2.37	0.29	0.52	0.07			M3	-4.8	272	
LMC 434	5 34 44.6	-65 6 39	17.69	4.00	0.48	0.70	0.00			M5	-5.2		low S/N
LMC 435	5 34 20.9	-65 31 35	16.39	4.32	0.31	0.63	0.22			M5S	-7.1	312	
LMC 441	5 31 16.9	-65 17 37	15.21	2.23	0.55	0.05	0.23			SC	-5.3	272	
LMC 444	5 30 49.1	-64 53 2	15.12	2.44	0.25	0.49	0.06			M3	-5.5	270	
LMC 445	5 28 48.0	-66 37 4	13.62	2.15	0.23	0.28	0.13			M1	-6.6	303	
LMC 446	5 28 43.9	-66 50 55	13.14	1.85	0.19	0.19	0.08			M0	-6.7	313	
LMC 447	5 28 50.2	-66 49 51	13.33	1.76	0.20	0.12	0.08			K5	-6.5	292	
LMC 448	5 28 49.1	-66 48 58	14.57	2.18	0.30	0.31	0.19			M1S	-5.7	271	
LMC 461	5 27 0.8	-67 3 12	13.04	2.19	0.24	0.19	0.11			M0	-7.2	236	
LMC VAR 41	5 23 19.2	-66 59 48	14.5	2.0	0.42	1.37	-0.16	0.40	1.71	>M6	-5.7:		V0 , (V-I)p=4.6
LMC VAR 19	5 40 39.3	-66 16 10	14.9	1.2	0.11	0.84	-0.15	0.15	0.98	>M6	-4.4	262	(V-I)p=3.4
LMC VAR 9	5 5 36.6	-66 7 22	16.9	4.0	0.06	0.04	0.03	-0.05	0.05	K4		71	galactic K giant
LMC VAR 44	5 25 27.2	-66 35 8	18.3	5.8	2.43	0.00	-0.35	4.34	2.40	>M6	-8.4		(V-I)p=5.8
LMC VAR 48	5 23 52.6	-66 44 7	14.7	2.5	0.20	1.27	-0.10	0.27	1.64	>M6	-6.1	311	(V-I)p=4.6
LMC VAR 43	5 26 11.6	-66 9 26	13.8	2.8	0.15	0.60	0.03	0.18	0.64	M4	-7.4	304	(V-I)p=3.3
LMC VAR 37	5 29 20.4	-67 4 48	17.6	5.1	-0.40	0.00	-0.37	1.24	2.15	>M6	-7.6	326	(V-I)p=5.6
BW 17	17 59 43.9	-30 5 42		5.5 p	0.37	0.84	-0.12	0.17	1.64	>M6			1
BW 86	18 0 6.2	-29 53 54		5.3 p	0.79	0.44	-0.18	0.34	1.17	>M6			1
BW 91	18 0 8.1	-29 54 40		4.2 p	0.25	0.34	-0.07	0.08	1.18	>M6			1
BW 212	18 0 43.0	-29 58 5		4.0 p	0.62	0.67	-0.05	0.39	1.02	M5			1
G1 866	22 35 50.3	-15 34 20	12.16	3.8	0.72	1.04	-0.14	0.27	1.15	>M6V		-66	M5 V
G1 884	22 57 36.2	-22 47 38	7.84	1.64	0.48	0.10	0.05	0.05	0.09	K5V		-13	M0 V
GJ 1247	19 54 35.0	-55 4 12	8.60	0.76	0.26	0.02	0.05	0.03	0.01	K4V		-6	K4 V
LMC R 1	5 42 52.1	-67 40 30	19.00	3.50	0.21	0.19	0.20	0.92	0.16	C	-3.5	427	Hα , V=396
LMC R 3	5 38 17.5	-66 8 52	19.00	4.50	0.42	1.49	-0.16	0.43	1.85	C	-5.2	330	
LMC J 4-9	5 16 53.0	-64 50 4		2.9 p	0.20	-0.28	0.21	1.46	0.34	C	0.0	323	J star,2
N419-25	1 6 13.0	-72 9 0		1.8 p	0.09	0.00	0.22	0.63	0.13	C	0.0	246	3
N419-16	1 6 13.0	-72 9 0		5.3 p	0.00	-0.01	0.11	-0.23	0.41	C	0.0	133	3
N1651-3304	4 37 12.0	-70 41 0		4.5 p	0.30	0.81	0.27	0.31	1.00	>M6S	0.0	223	4
WEST C-67	5 20 0.0	-66 48 0	13.80	1.47	0.18	-0.01	0.20	0.26	0.30	C	-5.3	353	5

OTHER LMC STARS AND STANDARD STARS—(*continued*)

STAR	RA (1950)	Dec	V	V-I	Na D	D(6180) TiO	D(6475) ZrO	D(5635) C2	D(7100) TiO	Sp	M(bol)	Vel	Remarks
DM+28 4592	23 27.2	28 59.5		2.1 p	0.22	0.23	0.31	0.04	0.18	M0S		-65	S
HD 24393	3 48 32.7	-60 16 10		1.80p	0.15	0.14	0.06	0.05	0.17	K5		-17	M0 III (LCO)
HD 24393	3 48 32.7	-60 16 10		1.80p	0.22	0.15	0.06			K5		-9	M0 III (AAO) template
G1 205	5 28 56.9	-3 42 12	7.96	2.08	0.68	0.32	0.00	0.00	0.00	M1V		36	M2 V
RZ SGR	20 11 34.8	-44 33 36		3.9 p	1.07	0.57	0.42	0.11	0.63	M4S		-43	Se + Li
VX AQUILAE	18 56 36.0	-1 38 0		5.6 p	2.57	1.00	0.23	0.11	0.31	C		-8	CS + Li
HD 195268	20 29 39.1	-68 42 15		2.3 p	0.20	0.36	0.06	0.07	0.33	M2		-29	M1 III, template
HD 182040	19 20 4.8	-10 47 13		1.3 p	0.17	-0.01	0.09	0.28	0.05	C		-9	C1,2 template
HD 25107	3 54.0	-69 33 0		1.9 p	0.31	0.15	0.07	0.02	0.12	K5		18	K5 III
HD 198064	20 46 15.3	-59 6 34		2.0 p	0.23	0.11	0.04	0.04	0.09	K5		3	K4 III, template
HD 197164	20 40.5	-55 45 0		0.8 p	0.11	0.02	0.03	0.04	0.05	<K4		-5	G8V
HD 196084	20 33.7	-53 15 0		0.9 p	0.02	0.02	0.04	0.01	0.02	<K4		45	G8 III
HD 196403	20 36.3	-64 22 0		0.9 p	0.21	0.03	0.04	0.04	0.03	<K4		2	G8 IV
DM-27 14351	19 49 37.0	-27 35 54			0.14	0.00	0.14	0.45	0.18	C		49	
NU PISC	1 38 49.7	5 14 5			0.16	0.05	0.00			K4		-6	K3 III
DM -2 891	4 21 51.2	-2 38 50			0.23	0.44	0.23			M3		11	M2S, template
DG ERIDANI	4 18 26.3	-16 56 56			0.25	0.55	-0.03			M4		113	M4 III
R Doradus	4 36 10.6	-62 10 36			0.57	0.92	0.00			>M6			M8e III
ETA 2 DOR	6 11 8.9	-65 34 38			0.24	0.32	-0.01			M1		45	M2S
R CMI	7 5 57.6	10 6 14			1.73	0.30	0.26			C		44	SC5-6
HR 2967	7 39 14.2	14 19 34			0.28	0.48	0.06			M3		-15	M3S
VYSSOTSKY 5	6 46 41.1	-20 22 8			0.22	0.64	0.11			M5		-19	M4S 6
NQ PUPPIS	7 50 43.7	-11 29 42			0.28	0.48	0.07			M3		-18	S4.5
LEE 5309	0 24 21.0	-72 5 13			0.13	0.06	0.03	0.01	0.37	K4		47	47 Tuc std, 7
LEE 4312	0 20 28.1	-72 3 54			0.07	0.02	0.05	0.02	0.03	K4		-44	47 Tuc std, 7
N288-20	0 50 14.0	-26 53 47			0.04	-0.01	0.03	0.02	-0.01	<K4		-44	NGC 288 std, 8
N288-33	0 50 26.0	-26 51 45			0.01	0.02	0.04	0.00	0.02	K4		-32	NGC 288 std, 8
M67-105	8 48 33.1	11 59 35			0.02	0.03	0.05	0.01	0.03	<K4		56	M67 std, 9, 10
M67-142	8 48 38.9	12 5 23			0.06	0.00	0.03	0.01	0.10	<K4		64	M67 std, 9
M67-226	8 48 49.0	11 57 43			0.04	0.02	0.04	0.02	0.12	<K4		17	M67 std, 9
West C67	5 2 56	-66 4 57											

REFERENCES.—(1) Blanco, McCarthy, and Blanco 1984. (2) Crabtree *et al.* 1976. (3) Lloyd-Evans 1980; Position quoted is cluster center. (4) Mould and Aaronson 1980; Position quoted is cluster center. (5) Westerlund *et al.* 1978. (6) Keenan 1954. (7) Lee 1977. (8) Cannon 1974. (9) Johnson and Sandage 1955. (10) Cohen 1980.

REFERENCES

Aaronson, M., and Mould, J. R. 1982, *Ap. J. Suppl.*, **48**, 161.
———. 1984, *Ap. J.*, **288**, 551.
Bahcall, J. N., and Soneira, R. M. 1980, *Ap. J. Suppl.*, **44**, 73.
Baldwin, J. A., and Stone, R. S. 1984, *M.N.R.A.S.*, **206**, 241.
Baud, B. 1982, in *Surveys of the Southern Galaxy*, ed. Burton and Israel (Dordrecht: Reidel), p. 165.
Becker, S. A. 1981, *Ap. J. Suppl.*, **45**, 475.
Bessell, M. S. 1979, *Pub. A.S.P.*, **91**, 589.
Bessell, M. S., and Wood, P. R. 1984, *Pub. A.S.P.*, **96**, 247.
Blanco, V. M., and McCarthy, M. F. 1983, *A.J.*, **88**, 1442 (BM83).
Blanco, V. M., McCarthy, M. F., and Blanco, B. M. 1980, *Ap. J.*, **242**, 938 (BMB80).
———. 1984, *A.J.*, **89**, 636.
Blanco, V. M., and Richer, H. B. 1979, *Pub. A.S.P.*, **91**, 659.
Cannon, R. D. 1974, *M.N.R.A.S.*, **167**, 551.
Cohen, J. G. 1980, *Ap. J.*, **241**, 981.
Cohen, J. G., Frogel, J. A., Persson, S. E., and Elias, J. H. 1981, *Ap. J.*, **249**, 481.
Crabtree, D. R., Richer, H. B., and Westerlund, B. E. 1976, *Ap. J. (Letters)*, **203**, L81.
Feitzinger, J. V., and Weiss, G. 1979, *Astr. Ap. Suppl.*, **37**, 575.
Freeman, K. C., Illingworth, G. D., and Oemler, A. 1983, *Ap. J.*, **272**, 488.
Frogel, J. A., and Blanco, V. M. 1983, *Ap. J. (Letters)*, **274**, L57.
Frogel, J. A., and Richer, H. B. 1983, *Ap. J.*, **275**, 84.
Gilmore, G. F. 1984, *M.N.R.A.S.*, **207**, 223.
Gilmore, G. F., and Reid, I. N. 1983, *M.N.R.A.S.*, **202**, 1025.
Glass, I. S., and Reid, I. N. 1985, *M.N.R.A.S.*, **214**, 405.
Iben, I., and Renzini, A. 1983, *Ann. Rev. Astr. Ap.*, **21**, 271.
Johnson, H. L., and Sandage, A. R. 1955, *Ap. J.*, **121**, 617.
Keenan, P. C. 1954, *Ap. J.*, **120**, 484.
Lee, S. W. 1977, *Astr. Ap. Suppl.*, **27**, 381.
Lloyd-Evans, T. E. 1980, *M.N.R.A.S.*, **193**, 87.
Mould, J. R. 1976, *Ap. J.*, **207**, 535.
———. 1983*a*, in *IAU Symposium 108, Structure and Evolution of the Magellanic Clouds*, ed. S. van den Bergh and K. S. de Boer (Dordrecht: Reidel), p. 195.
———. 1983*b*, *Ap. J.*, **266**, 255.
Mould, J. R., and Aaronson, M. 1979, *Ap. J.*, **232**, 421.
———. 1980, *Ap. J.*, **240**, 464.
———. 1982, *Ap. J.*, **263**, 629.
Pagel, B. E. J., Edmunds, M. C., Fosbury, R. A. E., and Webster, B. L. 1978, *M.N.R.A.S.*, **184**, 569.
Payne-Gaposhkin, C. 1971, *Smithsonian Contr. Ap.*, **13**, 1.
Ratnatunga, K. U., and Freeman, K. C. 1985, *Ap. J.*, **291**, 260.
Reid, N., and Mould, J. R. 1984, *Ap. J.*, **284**, 98 (Paper I).
Renzini, A., and Voli, M. 1981, *Astr. Ap.*, **94**, 175.
Stone, R. S., and Baldwin, J. A. 1983, *M.N.R.A.S.*, **204**, 347.
Weidemann, V. 1984, *Astr. Ap.*, **134**, L1.
Westerlund, B. E., Olander, N., and Heden, B. 1981, *Astr. Ap. Suppl.*, **43**, 267.
Westerlund, B. E., Olander, N., Richer, H. B., and Crabtree, D. R. 1978, *Astr. Ap. Suppl.*, **31**, 61.
Wood, P. R. 1981, in *Physical Processes in Red Giants*, ed. I. Iben and A. Renzini (Dordrecht: Reidel), p. 135.
Wood, P. R., Bessell, M. S., and Fox, M. 1981, *Ap. J.*, **272**, 99.
Wood, P. R., Bessell, M. S., and Paltoglou, G. 1985, *Ap. J.*, **290**, 477.

I. N. REID: Royal Greenwich Observatory, Herstmonceux Castle, Hailsham, East Sussex BN27 1RP England

J. R. MOULD: Caltech, 105-24, Pasadena, CA 91125